Physics – Uspekhi **60** (6) 539 – 558 (2017)

REVIEWS OF TOPICAL PROBLEMS

PACS numbers: 33.15.Pw, 33.50.Dq, 42.50.Ex, **61.46. – w**, 61.71.U – , 63.20.kp, 63.20.Pw, **78.55. – m**, **81.10. – h**

Vacancy–impurity centers in diamond: prospects for synthesis and applications

E A Ekimov, M V Kondrin

DOI: https://doi.org/10.3367/UFNe.2016.11.037959

Contents

Abstract. **The bright luminescence of impurity–vacancy complexes, combined with high chemical and radiation resistance, makes diamond an attractive platform for the production of single-photon emitters and luminescent biomarkers for applications in nanoelectronics and medicine. Two representatives of this kind of defects in diamond, silicon-vacancy (SiV) and germanium-vacancy (GeV) centers, are discussed in this review; their similarities and differences are demonstrated in terms of the more thoroughly studied nitrogen-vacancy (NV) complexes. The recent discovery of GeV luminescent centers opens a unique opportunity for the controlled synthesis of single-photon emitters in nanodiamonds. We demonstrate prospects for the high-pressure high-temperature (HPHT) technique to create single-photon emitters, not only as an auxiliary to chemical vapor deposition (CVD) and ion-implantation methods but also as a primary synthesis tool for producing color centers in nanodiamonds. Besides practical applications, comparative studies of these two complexes, which belong to the same structural class of defects, have a fundamental importance for deeper understanding of shelving levels, the electronic structure, and optical properties of these centers. In conclusion, we discuss several open problems regarding the structure, charge state, and practical application of these centers, which still require a solution.**

Keywords: high pressure, diamond, vacancy-impurity complexes, color centers, luminescence

E A Ekimov, M V Kondrin Vereshchagin Institute of High Pressure Physics, Russian Academy of Sciences,
Kaluzhskoe shosse 14, 108840 Troitsk, Moscow, Russian Federation
E-mail: ekimov@hppi.troitsk.ru, mkondrin@hppi.troitsk.ru

Received 20 July 2016, revised 31 October 2016
Uspekhi Fizicheskikh Nauk **187** (6) 577 – 598 (2017)
DOI: https://doi.org/10.3367/UFNr.2016.11.037959
Translated by S N Gorin; edited by A M Semikhatov

1. Introduction

Luminescence is a well-known physical effect, the study of which dates back to the classical work of Stokes published in the middle of the 19th century. According to the common definition, luminescence is any electromagnetic radiation from a substance carrying the energy that is higher than that of the thermal background. In this case, neither the aggregate state of the substance (the effect of luminescence can be related to separate molecules, liquids, and solids) nor the processes that lead to the luminescence are specified. We recall that in two well-known 'textbook' examples, namely, in the cases of the glow of white phosphorus and of ordinary sugar upon rubbing, luminescence occurs due to thermal and mechanical actions (thermo- and triboluminescence). At the same time, the simplest method for exciting luminescence (most convenient for studying this effect) is another electromagnetic radiation (photoluminescence), whose frequency can differ significantly from the characteristic frequency of the radiated light.

On the microscopic level, luminescence is caused by the transitions of electrons from the ground state to any excited level and by the subsequent relaxation of this excited state (effects connected with this process are considered in Section 5).

An important condition in this case is a comparatively long lifetime of this excited state (at least longer than the period of oscillations of the radiated light, which makes it possible to distinguish luminescence from the processes of light scattering). From the definition of luminescence, it follows that the excited level should be discrete, separated from the ground level by a gap. In the case of crystals, this condition is satisfied when there are impurity levels in the gap of semiconductors and dielectrics.

Owing to a wide band gap, diamond is transparent both in the visible and in the near-ultraviolet ranges and is an attractive 'platform' for studying luminescent centers. Systematic studies in this region started in the 1960s [1, 2]. At present, about 500 optically active centers are known in diamond [3, 4]. Although this number seems to be very large, it is comparatively small taking into account that this number includes *all* optically active defects.[1] In the crystal lattice of diamond, because of its rigidity and the relatively small interatomic distances, the formation of only a small number of simple types of defects is possible (such as vacancies and substitutional and interstitial impurities, which represent atoms with a small atomic radius). For the same reasons, a few more elaborate defect complexes can appear in the diamond matrix, consisting of one or several impurity atoms (even with a relatively large atomic radius) and of adjacent vacancies, which make it possible to incorporate such atoms into the diamond matrix. It is remarkable that just the small possible concentration of such complexes allows creating 'custom-made' optically active centers in nanodimensional materials, which are attractive from the practical standpoint (although the technology to create them proves to be relatively complex; see Section 3).

Interest in the defects that are present in diamond was until recently mainly connected with studies in fundamental or sufficiently specific applied fields (production of jewelry stones of uncommon color [5] or the study of geological conditions near the deposits of natural diamonds [6]). However, the recent rapid progress in high-resolution microscopy, biomedicine, biosensors, quantum information theory, and metrology, as well as the successes in the field of chemical synthesis of nanosize diamonds, has again drawn attention to this type of objects. In this review, we consider two comparatively 'young' representatives of impurity–vacancy centers, which, in spite of the difference in composition, belong to the same class of complexes, and also discuss the prospects for obtaining them and for their practical application.

2. New luminescent centers in diamond

In the last decade, optically active centers in diamond have become the subject of detailed study from the standpoint of the prospects for their use as luminescent markers in biology, for measuring weak magnetic fields with a high spatial resolution, and, most importantly, as so-called Λ systems (three-level quantum systems with two almost equally probable channels of relaxation of the excited state, which are considered in more detail in Section 9) and emitters of single photons for quantum computing and communication [7–16].

Of the 500 optically active centers existing in diamond, only about ten have so far found application as single-photon emitters [8]. In particular, the possibility was shown to use the centers of nitrogen-vacancy (NV) [9] and silicon-vacancy (SiV) [14] types, and also the centers connected with Cr [15] and Ni (NE8) [16]. The choice is narrow in and of itself, even if we take into account the possibility of creating new single-photon sources, which are considered below.

We note that the 'exotic' structure of the NE8 defect (a nickel atom surrounded by four nitrogen atoms) complicates the creation of single-photon sources with reproducible properties, and the structure of the Cr-containing center is not thus far established reliably, although it is assumed that oxygen participates in its formation. As regards applications in biomedicine, the presence of impurities of metals such as Ni, Cr, and Co in luminescent biomarkers is undesirable because these carcinogenic elements can be located on the surface of diamond particles and exert unfavorable influence on the subject of the study.

The most studied emitters of single photons are the NV and SiV centers, and the traditional methods of creating them are chemical vapor deposition (CVD) and ion implantation [7, 8]. At the same time, the development of technologies to create single-photon emitters based on NV and SiV centers has encountered serious difficulties in that nitrogen and silicon are the most common impurity elements in both natural and synthetic diamonds. Because of the high solubility of silicon and nitrogen in diamond, serious problems arise with the controlled introduction of SiV and NV centers in the process of growing crystals. Controlled doping becomes difficult to realize due to the impurities coming from the nearest neighborhood of synthesized diamonds. In the CVD processes, the source of the impurities of nitrogen and silicon is primarily the residual gases and quartz components of the reactors [17–19]. The low gas pressures employed during the synthesis (typically 30–100 Torr [20]) favor a rapid accumulation of uncontrollable impurities in the zone of the deposition of diamonds as a result of the high diffusive mobility of atoms and ions in the gas phase.

When using luminescent diamonds in biomedicine, the introduction of a dopant does not require delicate control. However, the CVD method does not ensure a reproducible synthesis of a large number of fine crystals necessary for application in medicine; under the conditions of a very low density of nucleation, separate diamond nanoparticles, inhomogeneous in size, are formed on the substrates [21]. The characteristic size required for this purpose is 5–100 nm [22, 23]. At the same time, obtaining nanodiamonds with a size less than the luminescence wavelength is very important for reducing losses arising upon reflection and refraction of light on the crystal boundaries and for increasing the efficiency of the collection of the emission of single-photon emitters [24].

Except for the uncontrollable introduction of nitrogen into diamond [25], the detonation technologies thus far are not a positive solution to the problem of obtaining doped

[1] The number 500 corresponds to the total number of impurity optical lines in the diamond described in Zaitsev's handbook [3], many of which, in all likelihood, correspond to different charge states of the same defect, which in many cases were obtained by quite 'exotic' methods. For example, the line at 1.979 eV can be mentioned, which is observed in implanted nitrogen-containing diamonds after their optical treatment at liquid nitrogen temperatures. In this case, the line at 2.367 eV fades and the line at 1.979 eV appears, which is apparently caused by a change in the charge state of some defect. This charge state is restored as the temperature increases to room temperature. However, if we consider only the centers with a technologically justified method for obtaining them, then their number turns out to be comparatively small, no more than several dozen.

nanodiamonds, and the crushing methods are inefficient because of the wide range of sizes of the synthesized particles. Problems also arise concerning the preservation of the structural quality of the initial diamond and the removal of grinding products; in addition, the nanoparticles obtained predominantly have the shape of fragments with sharp edges [26], which hampers their use in medicine.

Thus, on the one hand, the search continues for technological solutions with the purpose of controlling the doping process and improving the characteristics of NV and SiV centers with the use of methods of implantation, CVD, and detonation technologies; on the other hand, new optically active centers are synthesized and the technology of synthesis at high pressures is tested, aimed at solving the problems of improving the quality of the diamond 'platform' structure and the mass synthesis of doped nanodiamonds.

Recent reports on the use of the CVD method for obtaining new luminescent centers based on impurities of Ge [27–30] and Eu [31] in diamond open unique prospects for the direct synthesis of fine-size crystals of diamond with single luminescent centers due to the low equilibrium concentration of impurities. It is remarkable that in contrast to the nitrogen and silicon impurities, no structural impurities of germanium and rare-earth elements have been revealed in natural diamonds, although the oxides of rare-earth elements are frequent 'guests' in both carbonado polycrystalline diamonds and some types of single crystals [32, 33]. The impurities of germanium and rare-earth elements cannot be introduced unintentionally into the reaction volume when synthesizing diamonds. The interest in this property is quite significant because there appears to be an opportunity of controlled doping, which is difficult to realize in doping with nitrogen and with silicon.

The use of high pressures and temperatures (HPHTs) as a tool for the synthesis of diamonds with luminescent centers was until recently not regarded as the key approach to satisfy the needs of quantum electronics, although it was quite successfully used for restoring the structure and activating impurities after ion implantation [34, 35], improving the physicomechanical properties of CVD diamonds [36, 37], and modifying the range of colors of natural diamonds [38–40].

The stringent requirements for the quality of the structure when creating single-photon emitters make it necessary to turn to the synthesis of diamonds in the range of their thermodynamic stability. The perfection of the diamond structure can be estimated from the width of the line of Raman scattering (RS) of light at 1332 cm^{-1}, because the presence of defects leads to an asymmetric broadening of this line. The comparative study of the structure of natural, CVD, and HPHT diamonds has shown that for diamonds obtained in the CVD process, the characteristic width of the RS line is usually 2.3–7.8 cm^{-1} [41], whereas in diamonds synthesized at high pressures it is usually about 1.7 –2.2 cm^{-1}. It is the HPHT diamonds that are used as substrates for growing high-quality single crystals in the CVD process [42]. In this case, the structural quality of the films obtained by the CVD method is lower than the perfection of the HPHT substrates [43]. We emphasize the fundamental differences between the HPHT and CVD methods of growing diamonds. In the HPHT method, the diamond is formed under thermodynamically equilibrium conditions, whereas in the CVD method it grows under metastable conditions; moreover, the presence of atomic hydrogen in the growth plasma is a fundamental condition that ensures the removal of sp^2 hybridized carbon formed in the process of growth.

As regards the synthesis of nanodiamonds at high static pressures, the first report on their synthesis from organic compounds by Wentorf appeared more than half a century ago [44]. At that time, this discovery did not find a proper use. Obtaining doped nanodiamonds is a new direction in the synthesis of nanodiamonds from organic compounds, whose development was stimulated by the necessity of solving the problem of the creation of luminescent diamonds with a highly perfect structure.

The primary focus in this review is on impurity–vacancy complexes, by which we understand complex defects that consist of a single impurity atom and one or more nearest vacancies. Historically, the first example of such complexes was the nitrogen complex NV, which is encountered in natural diamonds. Artificial complexes with silicon were first obtained in 1980 by Vavilov et al. [45] in the first experiments on growing CVD diamonds. Although the participation of silicon in the formation of these defects was established practically immediately, attempts to explain their structure continued for almost 15 years, until Goss [46] proposed a structural model in 1996, which triggered research on a class of vacancy complexes that were called split-vacancy complexes.

As the initial model, Goss took the model of the NV complex in which one of the carbon atoms was replaced by a silicon atom, and the adjacent site contained a vacancy (the symmetry of such a center is C_{3v} or 3m; the center of inversion is absent). The optimization of the chemical bonds of this structure using the density-functional theory (DFT) leads to the 'pushing-out' of the impurity atom of silicon to almost the center of the bond that connects its initial position with the adjacent vacant site. In this case, it turns out that the inversion symmetry of the center (D_{3d} or $\bar{3}$m) is restored with good accuracy, and the silicon atom turns out to be located as if between two vacancies, giving rise to the appearance of the general name (split-vacancy complex) for defects of this type. Subsequently, Goss [47, 48] considered in detail all possible combinations of Group IV and Group V elements that can form both complexes of this type and more complex vacancy complexes including more than two vacancies; however, most of them cannot thus far be synthesized, except for the GeV complex, which was obtained experimentally in 2015 as a result of CVD synthesis [27, 28] and HPHT synthesis [29, 30].

We also note that more elaborate vacancy complexes are considered possible candidates for creating defects of larger volumes (nanopores), into which atoms with a substantially larger atomic radius (for example, europium [31]) could be introduced; however, this problem is rather hypothetical in nature at present, and we do not discuss such elaborate complexes here.

From the practical standpoint, interest in SiV and GeV centers (just as in the NV center) is due to their optical properties, because they form impurity levels in the forbidden gap of diamond, which demonstrates sufficiently bright and practically monochromatic luminescence. In advanced developments in quantum communication, metrology, and quantum informatics, centers of this type are considered possible candidates for the role of single-photon sources, and interest in sources of this type increases significantly if some uncommon interactions are revealed in them between electrons or electron spins, and also between emitted or

absorbed photons (for example, in quantum-entangled electron–photon states in NV centers, which are considered in detail in Section 9).

The study of split-vacancy impurity centers, in contrast to the study of NV centers, is currently only at the beginning, which is partly explained by their comparative 'youth.' This is to a certain extent reflected in the number of reviews concerning impurity centers in diamonds: several fundamental reviews are devoted to the NV centers (e.g., [49, 50]); for the SiV centers, only Hepp's PhD thesis (2014) can be regarded as such a review [51]. To a certain degree, we hope that our review will fill some gaps in the literature on split-vacancy centers.

We examine the state of the art in the specified areas of studies in more detail. When considering methods for creating optically active centers in diamonds with the use of CVD and ion implantation, the primary attention is given to the prospects of using annealing at high pressures for modifying the structure and properties of the diamond.

3. Methods for creating impurity centers and sources of single photons

3.1 Ion implantation

The method of ion implantation is widely used for obtaining semiconductor structures, for example, on silicon substrates [52–54]. The method includes the ionization of impurity atoms and ion bombardment of the substrate (target) in an accelerating electric field. The characteristic depth of the penetration of impurity ions into the substrate ranges from several hundred nanometers to several micrometers. The ion bombardment is accompanied by the formation of structural imperfections, mainly vacancies and interstitial atoms and ions. On the whole, the degree of damage to the structure is determined by the type and kinetic energy of the implanted ions and by the radiation dose. Subsequent high-temperature annealing (at 800–1100 °C) is used not only to restore the violated structure but also to 'activate' the impurity. For example, in the case of an electrically active impurity, 'activation' implies the recombination of interstitial atoms and vacancies with the formation of a substitutional impurity. In contrast to silicon, diamond has a substantially higher Debye temperature and is a metastable phase at normal pressures. At a threshold concentration of vacancies (10^{22} cm^{-3}) created during the implantation, the structure of diamond cannot be restored; the appearance of the graphite phase is observed upon annealing at temperatures above 800 °C [55–57]. Even in the case of smaller doses of implanted ions, it is not possible to completely rule out the possibility of the local formation of a nondiamond modification of carbon upon annealing.

The 'activation' of an impurity, i.e., placing the impurity in a lattice site or the formation of complexes with the participation of vacancies, also greatly depends on the annealing temperature if the vacancy (vacancies) and the impurity atom (ion) are within the limits of a single diffusion hop. On the whole, the diffusion mobility of impurities in diamond at temperatures that correspond to restoration annealing is strongly suppressed. Discussions of the diffusion of atoms in diamond can be found in [35, 58, 59]. As a result of the study of the concentration profile of ^{13}C at the boundary of a diamond 'sandwich' obtained by the deposition of a diamond layer of ^{13}C atoms onto the surface of natural diamond (the base of ^{12}C atoms), it has been shown that the depth of penetration of the ^{13}C carbon isotope into the diamond after annealing for 20 h at a temperature of 1800 °C under a pressure of 7.7 GPa does not exceed 32 nm [58]. The diffusion coefficient of ^{13}C in diamond at 1800 °C is estimated to be not greater than 6×10^{-19} cm^2 s^{-1} (see the Table).

Table. Calculation of the self-diffusion coefficient D of carbon in diamond based on experimental data at a pressure of 7.7 GPa [58].

T, °C	D, cm^2 s^{-1}
2300	2.8×10^{-17}
2000	8.5×10^{-18}
1800	5.9×10^{-19}

When using the method of the preliminary introduction of boron into diamond by implantation [35, 59], the annealing of samples at 1300–1650 °C for 1 h does not lead to a noticeable migration of boron in the diamond; the degree of activation in this case is less than 1% (Fig. 1). The degree of activation of the same order of magnitude is experimentally observed for NV centers upon the implantation of nitrogen [60], and a similar degree of activation can be expected for SiV and GeV centers. It is assumed that the factor responsible for the inefficient activation of the impurity is the competing recombination of vacancies and 'supplanted' carbon atoms and also the formation of complicated complexes that block the vacancies. The use of high pressures can retard the graphitization of diamond, but even after annealing at a pressure of ≈ 7 GPa and temperatures of 1400 °C, the efficiency of the activation of the implanted impurity, e.g., boron, is quite limited, at the level of 7% [35]. The mechanism underlying the effect of pressure on the activation of impurities remains unclear. In the case of implanted nitrogen, an HPHT annealing of diamond substrates does not give any special advantages upon the activation of NV centers and requires a quite delicate choice of conditions, which is connected with the dissociation of the NV centers and the formation of nitrogen pairs at high temperatures (≈ 2000 °C [61]) (Fig. 2).

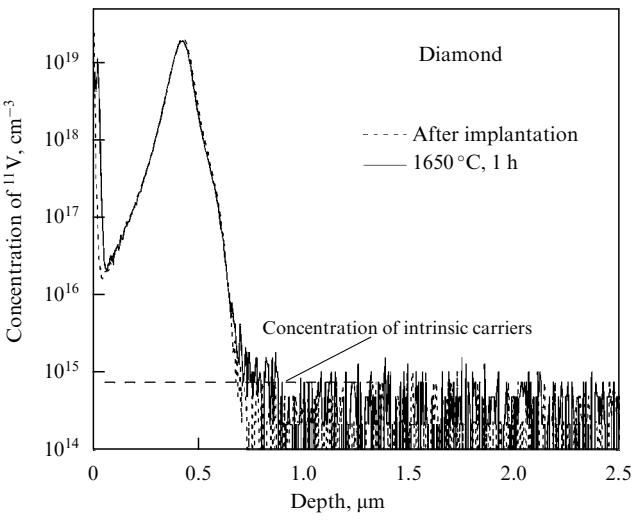

Figure 1. Boron concentration distribution established by secondary-ion mass spectroscopy (SIMS) along the direction of implantation before annealing (dashed curve) and after annealing at a temperature of 1650 °C for 1 h (solid curve) [59].

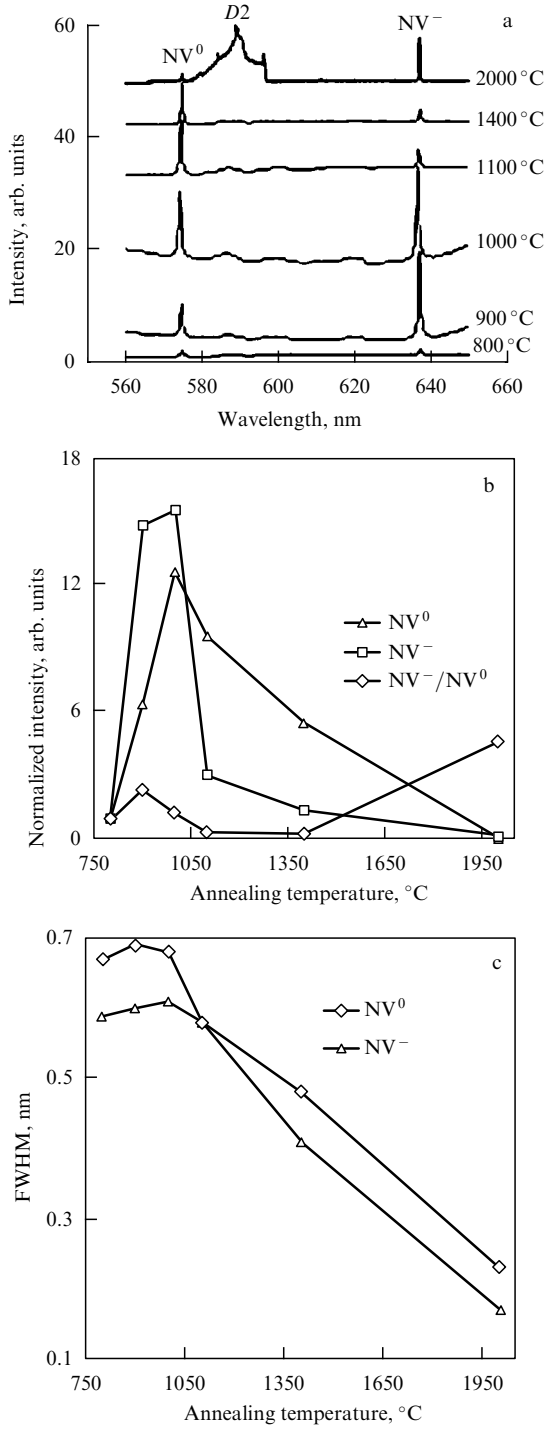

Figure 2. Effect of the annealing temperature on the intensity of luminescence of NV^0 and NV^- defects in diamond that were obtained by ion implantation into a CVD single crystal [61]: (a) luminescence spectra obtained after annealing at 800–1400 °C in a vacuum and at 2000 °C and a pressure of 8 GPa (the scale of the spectrum is increased by a factor of 10; D2 is the group of second-order RS lines in diamond); (b) normalized intensities of luminescence of NV^0 and NV^- defects and the ratio of these intensities (NV^-/NV^0) depending on the treatment temperature; and (c) temperature dependence of the full width at half-maximum (FWHM) of the luminescence lines of NV^0 and NV^- defects.

The above data give an idea of the complexity and ambiguity of the results of experiments on the creation of defects in diamond by ion implantation. It is important that 'nonactivated' impurities, which appear to be present in the form of complicated complexes, become a source of practically indestructible structure distortions. The covalent radius of nitrogen does not exceed that of carbon, which implies that nitrogen is located in the substitutional position upon the dissociation of NV centers. As regards the vacancy complexes of Si and Ge (as well as of Eu and Er, if such complexes exist), the vacancies in them are 'glued' to an impurity with a radius that is greater than that of carbon; the stable existence of the impurities of Si and Ge (Eu and Er) in the substitutional or interstitial state is energetically unfavorable [31, 47]. Hence, the HPHT annealing of diamond at temperatures above 2000 °C can be implemented without the risk of dissociation of the SiV and GeV complexes; however, no relevant experimental results have yet been published.

3.2 Chemical vapor deposition

Obtaining sources of single photons in diamond by the CVD method is considered in several rather detailed reviews (see, e.g., [8, 49]). During the CVD process, the growth of films in the presence of impurities of N, B, Si, Ge, etc. is accompanied by the incorporation of atoms into the diamond lattice in the form of a substitutional impurity and various complexes, including those with the participation of vacancies. As regards the creation of optically active NV and SiV centers in a nanodiamond by the CVD method, the uniformity of doping, the reproducibility of the results, and the output of doped nanodiamonds are on a low level [47]. The last is the natural limitation of the method of growth on substrates. If it would be possible to carry out the synthesis of nanodiamonds in the gas phase on levitating crystallization centers, such a process could solve the problem of mass production of CVD nanodiamonds. The spectral width of the lines of single-photon emitters in CVD nanodiamonds is noticeably wider than in macroscopic crystals; the reasons for such a broadening remain thus far unclear. It can be assumed that upon incorporation of impurity atoms into the diamond lattice under metastable conditions, structural imperfections with sp^2 hybridized carbon can arise, which can be responsible for the appearance of mechanical stresses. Nanodiamonds are usually obtained at reduced temperatures [62], which contributes to an increase in the number of defects because of the low mobility of atoms in the growing layer. The possible presence of sp^2 carbon atoms follows from the appearance of a dark brown color of the diamond intentionally doped with nitrogen in the process of its deposition [37] (Fig. 3). Upon subsequent annealing at pressures of 7 GPa and temperatures up to 2200 °C, the crystals became more transparent, their color changed to blue-grey, and then they became colorless. The overall nitrogen content in the diamond, just as its concentration, did not change. Annealing at temperatures around 1900 °C led to the transformation of the NV centers into other defects, supposedly into NVN or NNNV (i.e., consisting of one vacancy and two or three adjacent impurity atoms). At 1900 °C, a dissociation of the NV centers occurred, which was accompanied by the migration of vacancies; at higher temperatures, of the order of 2200 °C, the formation of nitrogen pairs was detected. It is interesting that the structure and content of hydrogen-containing defects in the diamond lattice then remain unaltered, which allows regarding the presence of 'hydrogen' defects as a characteristic feature of CVD diamonds.

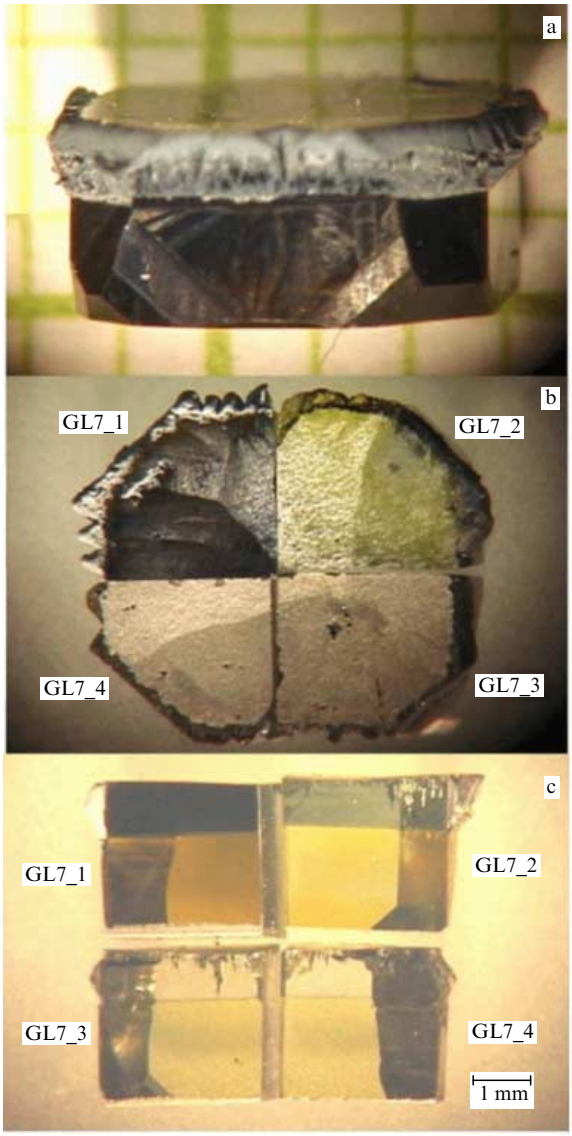

Figure 3. (Color online.) Variation of the color and transparency of a diamond crystal grown by the CVD method on a substrate of an HPHT diamond single crystal depending on the conditions of annealing under a pressure of 6.5–7 GPa [37]: (a) initial CVD crystal on a substrate; (b, c) quarters of the initial crystal on the substrate: (b) prior to and (c) after the annealing; GL7_1, initial crystal on the substrate; GL7_2, crystal after annealing at 1900 °C (1 h); GL7_3 and GL7_4, crystals after annealing at 2200 °C for 1 h and 10 h, respectively.

3.3 Synthesis at high pressures and high temperatures

It is known that synthesis at high pressures in the stability range of diamond allows obtaining diamonds with a high perfection of the crystal structure. For example, the growth of diamond crystals on a substrate in a metal melt containing silicon allowed studying the fine structure of lines in the luminescence spectra of a SiV center at wavelengths of about 737 nm [63, 64]. The observation of the isotope-related separation of luminescence lines made it possible to reliably connect the nature of the center responsible for the luminescence with impurities of silicon [64].

In this section, we discuss the problem of synthesis of diamond with optical centers in nonmetallic growth media. In contrast to the crystal growth of diamond in traditional solvents of carbon based on transition metals, such as Fe, Co, Ni, Cr, and Mn [65], synthesis in nontraditional growth media, such as C–H (hydrocarbons) [44], C–P [66], C–S [67], C–B_4C [68], and C–H_2O [69], allows doping diamond without the risk of magnetic metallic inclusions and impurities forming, whose presence not only worsens the structure of diamond but also has a negative effect on the stability of the spin states of optical centers. When applying luminescent diamonds as biomarkers in medicine, the presence of metals is also undesirable.

Synthesis in nontraditional media typically occurs at higher temperatures and frequently leads to obtaining new impurity states. The synthesis in binary systems is especially attractive from the standpoint of explaining the results obtained. For example, in the case of the synthesis of diamond in the B–C system [68], samples heavily doped with boron can be obtained (with the boron concentration in diamond around $10^{21}\,\mathrm{cm}^{-3}$) due to an increase in the solubility of boron in diamond at temperatures close to the melting point of the boron carbide–graphite eutectic (2500 K). The synthesis of diamond in the C–N [70] and Ge–C [71] systems was successfully realized, whereas in the Si–C system only silicon carbide SiC was formed, which is stable at temperatures up to about 3100 K at pressures up to 8–9 GPa [72]. The synthesis of well-faceted diamonds in the C–N system was realized using the decomposition of graphite-like C_3N_4 at pressures of 22 GPa and temperatures higher than 1000 °C [70]. At such high pressures, which correspond to the direct transition of graphite into diamond, polycrystalline nanodiamonds formed from graphite [73]. Although nitrogen does not manifest catalytic properties with respect to the synthesis of diamond [44], its presence as the 'ballast' in the initial 'graphite' prevents the sintering of diamond particles and favors the appearance of faceting. In [44, 70], the luminescence of crystals was not studied, although the temperatures of the synthesis were favorable for the formation of NV centers.

The catalytic properties of germanium in transforming graphite into diamond (in growing diamond crystal seeds in a germanium melt) were demonstrated quite long ago [71], but the study of optical properties was not a priority in [71]. The formation of GeV centers in diamonds grown in a binary Ge–C system under pressure was observed later [29], already after the discovery of GeV centers in CVD diamonds and in diamonds implanted with germanium [27]. From the applied standpoint, the synthesis of diamond from a germanium melt under pressure appears to be of little interest. The presence of inclusions of germanium in diamond causes the appearance of significant mechanical stresses, which can lead to the destruction of crystals [30] (Fig. 4): the volume of germanium increases during the solidification, which becomes critical for obtaining crystals with high optical quality.

More promising from the practical standpoint of growth were ternary systems such as dopant–C–H. By varying the initial composition, it is possible to control the level of doping, avoiding the formation of inclusions of the dopant. Microcrystals of diamond doped with Si, N, and Ge have been obtained at pressures of 8–9 GPa from mixtures based on naphthalene ($C_{10}H_8$) [30, 74].

3.4 Synthesis of nanodiamonds with SiV, NV, and GeV centers at high pressures and temperatures

The methods of the mass synthesis of nanodiamonds such as the detonation and laser ones are dynamic synthesis methods that take a short time (several milliseconds) under strongly nonequilibrium and poorly controlled temperature and

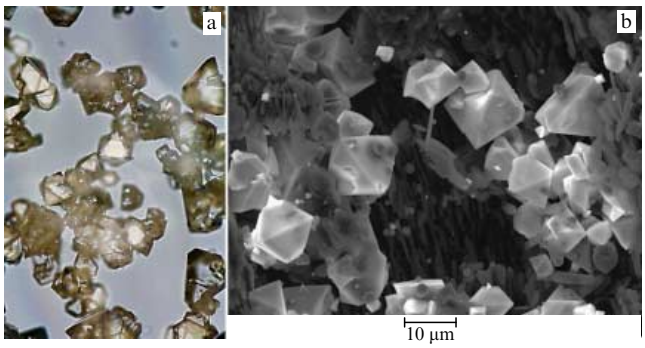

Figure 4. Diamonds synthesized in a C–H–Ge system at a pressure of 8–9 GPa and a temperature of 1600 °C from a mixture of naphthalene and germanium: (a) optical image and (b) electron-microscopic image [30].

pressure conditions. It follows from the experience on the synthesis of doped diamond under static conditions that the structural state of an impurity and its concentration in diamond depend not only on the composition of the growth medium but also on the synthesis parameters. For example, an increase in the synthesis temperature leads to the aggregation of nitrogen impurities and a reduction in their general concentration in diamond [75]. Until now, the problem of obtaining doped nanodiamonds was solved with the use of a top–down approach, which consists in the mechanical milling of the doped bulk diamond obtained by static synthesis methods such as CVD and HPHT [26, 76]. This approach is multistage and very expensive. The process of milling is accompanied by the contamination of diamond by metals, as well as by its graphitization. Furthermore, it is known that mechanical milling always leads to the appearance of structural defects in the near-surface layers of particles, which becomes critical when creating single-photon emitters. The resulting product of milling — diamond nanoparticles with a polydisperse size distribution — have the form of fragments with sharp edges as a result of the fracture on cleavage planes (111) (Fig. 5), which is extremely undesirable for their use in medicine. In addition, the yield of small-size nanoparticles is extremely low in this case.

The method of synthesis of nanodiamonds from organic compounds realized at high pressures by Wentorf more than half a century ago [44] is now increasingly in demand for obtaining nanocrystals of diamond with optically [7–16] and electrically [77, 78] active impurities for use in biomedicine and nanoelectronics. In [44], at pressures of the order of 14 GPa and temperatures near 1300 °C, an extraordinarily 'soft' diamond was obtained (not scratching glass, which possibly indicated the absence of scratches visible to the eye); the broadening of its X-ray diffraction lines was also noted, which indicated the formation of diamond in a nanocrystalline form. Later, it was shown in [79] that nanodiamonds can be obtained at lower pressures and temperatures than those used by Wentorf. Undoped nanodiamonds were obtained at a pressure of 8 GPa and temperatures of 800–1300 °C from camphene ($C_{10}H_{16}$). According to the data of transmission electron microscopy (TEM), the sizes of elementary crystallites did not exceed 10 nm. We also note a recent study on obtaining diamond nanocrystals with a size of several nanometers in the C–N system (by the decomposition of C_3N_4) [70]. The very high synthesis pressure (15–25 GPa) and small dimensions of the

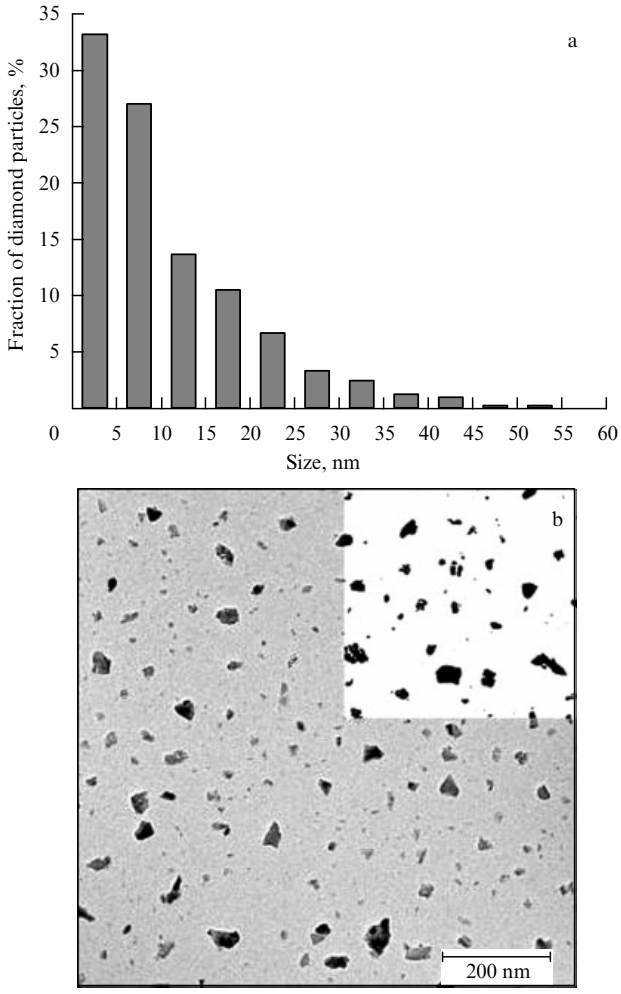

Figure 5. (a) Size distribution of diamond particles obtained by milling an HPHT diamond and (b) their shapes [26].

platinum capsule for the preparation of samples rule out the practical importance of this method of diamond synthesis.

The first reports on the synthesis of nanodiamonds with SiV, NV, and GeV centers at high pressures came from the Vereshchagin Institute for High Pressure Physics, Russian Academy of Sciences. The nanodiamonds were obtained using naphtalene-based mixtures at pressures of 8–9 GPa. Although the fraction of nanodiamonds in the mixture with microcrystals was insignificant (5%), their structure, in contrast to that of CVD diamonds, was virtually no worse than that of bulk crystals [30, 74, 80]. As a consequence, the narrowest spectral lines of SiV centers were obtained in HPHT nanodiamonds [80] (Fig. 6). The question of the mass synthesis of nanodiamonds with SiV, NV, and GeV centers has not been answered to date. The literature data on the synthesis of nanodiamonds (including doped nanodiamonds) at high pressures are quite scarce. In contrast to the synthesis of micro- and nanodiamonds from mixtures of reagents based on naphthalene with a planar structure of the molecule, the synthesis of diamonds via the decomposition of the individual compound 9BBN (9-borabicyclononane) with a bridge-type structure and boron atoms in the carbon cycle occurs with the formation of only a nanodiamond component with a boron impurity in the diamond lattice [78, 81] (Fig. 7). Obtaining nanodiamonds doped with boron at a pressure of 8–9 GPa and temperatures of 1000–1400 °C is the first

promising result in the field of the mass synthesis of doped nanodiamonds at high pressures.

At the same time, problems concerning the mechanism of the formation of nanodiamonds from organic compounds at pressures *below the pressure of the direct transition of graphite into diamond* (10–11 GPa [82, 83]) and of the doping of nanodiamonds with impurities remain unsolved, which does not permit predicting the conditions necessary for its synthesis. In a few studies concerning the synthesis of undoped nanodiamonds [44, 79, 84] using organic compounds, assumptions were made on the key role of the structure of the initial compounds in the formation of diamond nuclei: the structures of saturated hydrocarbons (paraffin, polyethylene) and of cyclic compounds with carbon bridges (adamantane, camphene) with sp^3 hybridized carbon atoms favor the formation of diamond, whereas the planar structure of aromatic compounds (naphthalene, anthracene) stimulates the formation of perfect graphite, which hinders the formation of diamond. In Ref. [84], the atomic ratio H:C (1.6–0.03) in the initial hydrocarbons was suggested as a condition favorable for the formation of diamond. Apart from the effect of hydrogen on the formation of diamond from organic compounds, it is noted that the presence of a noticeable amount of nitrogen in the structure of organic compounds is favorable for the formation of graphite and is unfavorable for the synthesis of diamond; the role of oxygen is not clear, but its presence does not block the process of the formation of diamond [44].

The recent results on obtaining nano- and microcrystals of diamond in samples consisting of a mixture of naphthalene and fluorized graphite were explained by the formation of particles of nano-onion and microsize platelet graphite at the intermediate stage of the transformation, whose size is inherited by the diamond particles [85]. We note that the idea of the key role of nanographite in the synthesis of nanodiamonds was suggested earlier when studying the behavior of individual organic compounds [84] and carbon

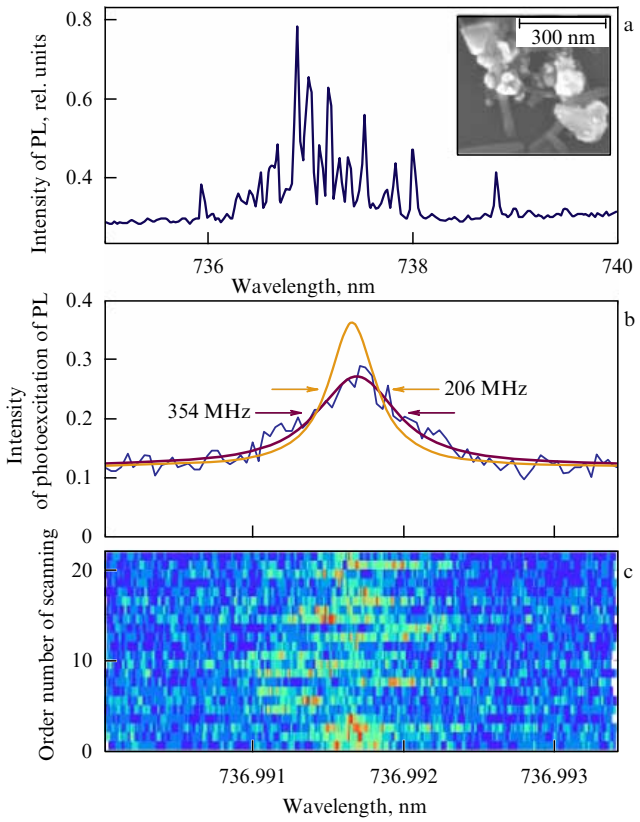

Figure 6. (Color online.) Resonance excitation of individual SiV centers in diamond: (a) photoluminescence (PL) spectrum of nanodiamonds with a size of less than 200 nm (in the inset, an SEM image demonstrating the occurrence of several centers); (b) spectrum of a center obtained by the photoluminescence excitation (PLE) method (linewidth 353 MHz); (c) with corrections taking the shifts of some scans into account, the width of the line is equal to 206 MHz (the curve with the highest peak in Fig. 2b), which corresponds to the lifetime of the excited state [80].

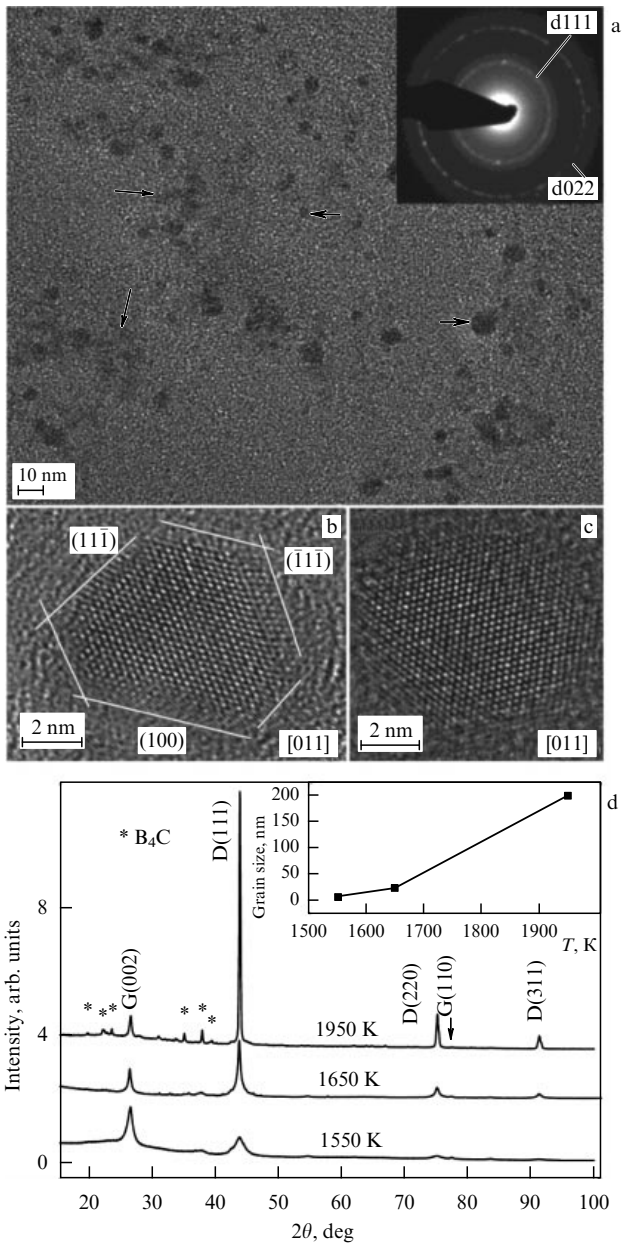

Figure 7. Synthesis of nanodiamonds doped by boron from the organoboron compound 9-BBN ($C_{16}H_{30}B_2$) at pressures of 8–9 GPa and temperatures of 1550–1950 K [78]: (a–c) images of nanocrystals obtained by the method of transmission electron microscopy (TEM) (in the inset in Fig. 6a, the electron diffraction pattern is given; d111 and d022 are the diffraction reflections of diamond); (d) diffractograms of samples synthesized at different temperatures (in the inset in Fig. 6d, the effect of the synthesis temperature on the size of obtained nanocrystals is shown). G — graphite; D — diamond.

materials [86]. In [86], the focus was on the synthesis of nanodiamonds at pressures exceeding that of the direct transition of graphite into diamond. On the whole, the proposed correlations are not general, and in the literature there are numerous controversies related to the behavior of the same organic substance at high pressures and temperatures. In this connection, systematic studies of the regularities in the high-pressure decomposition of individual organic compounds that contain dopant atoms, and also the study of the structures and composition of the resultant carbon materials, remain important for explaining the mechanisms of synthesis and doping of nanodiamonds.

3.5 Synthesis of diamonds with impurities of germanium and rare-earth elements

The detection of luminescence at a wavelength of approximately 602 nm in the spectra of a diamonds doped with germanium, reported in [27], generated enormous interest, as was mentioned in Section 2, in connection with the opportunity to solve the problem of controlled doping and obtaining nanocrystals with single luminescent centers directly in the process of synthesis. It was shown that the center at '602 nm' is formed in diamond films grown in the presence of germanium and in diamond implanted by germanium after its annealing [27] (Fig. 8). It was established that the luminescent center at '602 nm' has all the properties of a single-photon emitter, although the nature of the center remained open to debate because of the low quality of the luminescence spectra and the presence of uncontrollable impurities in the diamond, in particular, nitrogen and silicon. In later studies [28, 29] devoted to the doping of diamond with germanium, in particular, at high pressures [29], it was impossible to solve the fundamentally important problem of the nature of the luminescent center at '602 nm.' No isotopic separation of the zero-phonon line (ZPL) occurred in the spectra of GeV centers in diamond at low temperatures, while in the spectra of SiV centers the ZPL becomes split at low temperatures. To explain the nature and the structure of 'germanium' centers, a synthesis of diamonds was developed with the use of isotope-enriched germanium (^{72}Ge, ^{76}Ge) and carbon (^{12}C, ^{13}C) in the ternary Ge–C–H and quaternary Ge–C–H–O systems under conditions where germanium was an additive rather than a solvent of carbon [30]. According to the observation of shifts in the fine structure of the ZPL, the 'germanium' nature of luminescence was unambiguously established at the wavelength of 602 nm [30]. On the whole, the width of this luminescence line did not depend on the size of the synthesized crystals, which indicates a high structural perfection of the nanodiamonds obtained. Depending on the conditions of their synthesis, the diamond crystals could contain silicon and nitrogen impurities. In that case, the nitrogen centers were revealed only upon cooling. The addition of boron to the system led to the binding of the impurity nitrogen and disappearance of the luminescence lines of nitrogen centers. The source of silicon and SiV centers in diamond proved to be the agate mortar that was used to prepare the mixtures of reagents. The replacement of the agate mortar by a plastic mortar and of the elements of the high-pressure cell by elements that did not contain silicon solved the problem of the incorporation of silicon into diamond.

Thus, the method of high pressures makes it possible to sufficiently easily and reliably control the conditions of doping. As regards the concentration of GeV centers in diamond, its determination is a very complex issue in the absence of suitable reference samples. The germanium concentration in CVD films determined by the method of secondary-ion mass spectroscopy is at the level of 10^{16} cm^{-3}. The concentration of germanium in the reaction mixture was maintained by the interaction of microwave plasma with germanium in the solid state. For comparison, the concentration of the impurity silicon, which was not specially introduced into the reactor, was of the order of 10^{18} cm^{-3}. In [29], the overall concentration of germanium in the HPHT diamond determined by the mass spectroscopy method was in the range from 1 ppm to several hundred ppm (10^{17} – 10^{19} cm^{-3}). The data obtained do not seem to give the real concentration of GeV centers in the diamond lattice and are apparently significantly overstated because of the presence of germanium-based inclusions and clusters. The estimate of the concentration of GeV centers with the use of data on the absorption of samples and on the concentration dependence of the absorption of diamond with SiV centers gives a value that does not exceed 5×10^{14} cm^{-3} [30]. If this is so, then crystals with single luminescent centers — an ideal source of single photons — can be obtained by synthesizing diamonds less than 100 nm in size.

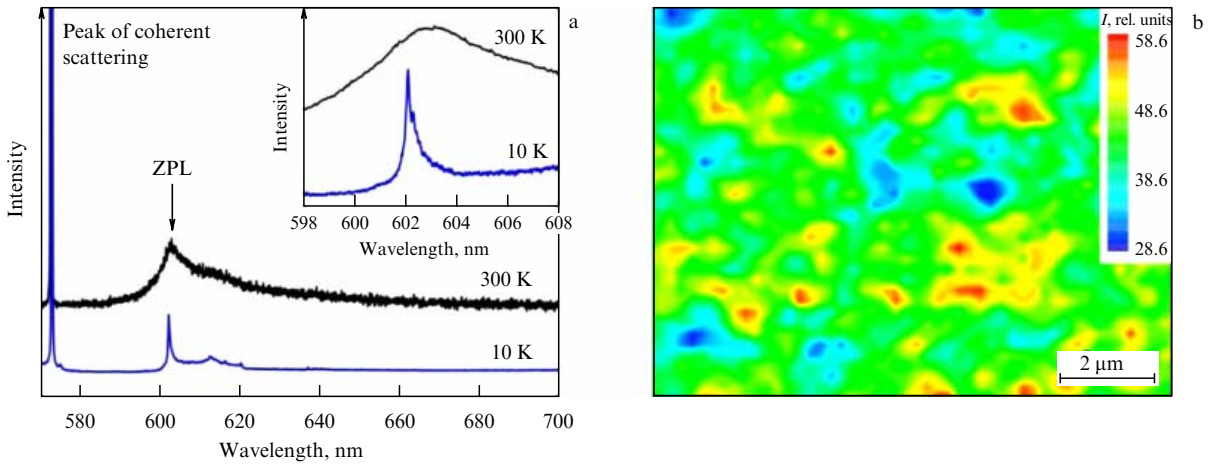

Figure 8. (Color online.) (a) Luminescence spectra of diamond with a GeV center obtained by the implantation method. The inset shows the ZPL; (b) intensity (shades of grey) of the ZPL scanned over the implanted surface [27].

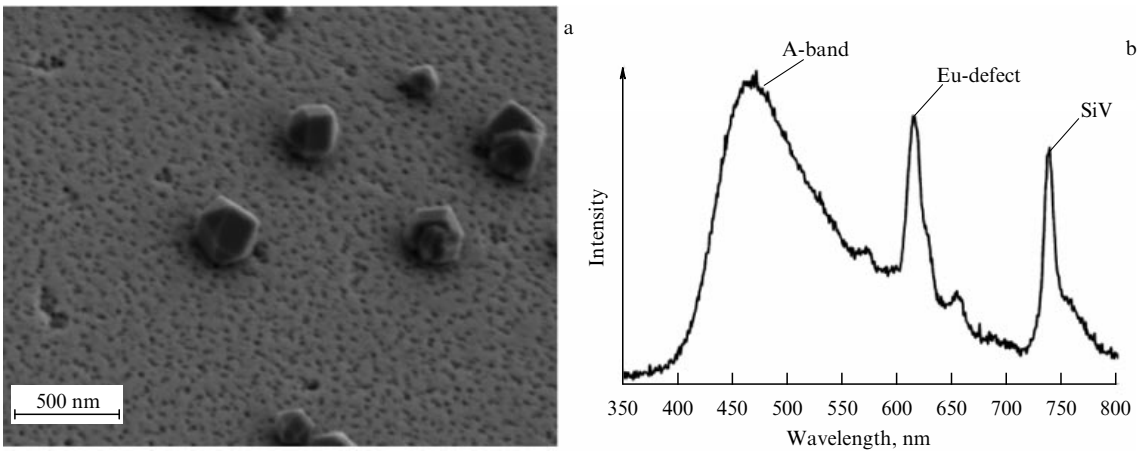

Figure 9. (a) Microstructure of diamond and (b) cathode luminescence of an Eu defect in a nanodiamond [31].

In our study [30], the luminescence on microcrystals and aggregated nanocrystals was discussed; currently, the luminescence on individual nanocrystals is being studied.

Obtaining rare-earth-element luminescent centers in diamond has long attracted the attention of researchers. A breakthrough in this area would allow the high chemical stability of diamond to be combined with the very prolonged coherence time of the nuclear spin of rare-earth ions (quantum memory, magnetic sensors) and with their bright and narrow luminescence in practically all spectral ranges that are needed. For example, there is a patent on obtaining (by the method of implantation) erbium-based luminescent centers with the emission wavelength of 1.5 μm, which would be ideal for the transfer of signals using quartz fibers [87]. However, publications that could confirm the data of this patent on the creation of erbium-based luminescent centers in diamond films by the method of implantation are absent. On the whole, it is noted in the literature that the methods of implantation of impurities of rare-earth elements into diamond do not lead to the formation of luminescent centers because of the graphitization of diamond at the stage of the subsequent annealing for restoring the diamond structure [31]. There is a paper on obtaining bright luminescence of Eu^{3+} ions 'fixed' in Eu–O–C bonds on the surface of particles in ultradisperse diamond powders [88]. The luminescent centers with such a structure can have only a very limited application.

The most interesting result concerning obtaining luminescent centers on the basis of rare-earth elements in diamond was published in [31]: Eu^{3+} was introduced into the diamond lattice of films and nanocrystals in several stages in a complex process, which included the oxidation of the surface of a diamond film, the chemical deposition of europium, and the subsequent overgrowth of a diamond layer. Luminescence was observed in the region of approximately 600 nm (Fig. 9). This result is of fundamental importance even in the absence of a practical application: the luminescent centers of a rare-earth center can be created in the process of the growth of diamond. However, there are no papers about the synthesis of diamond with the impurities of rare-earth elements yet.

4. Optical properties, electron structure, and the charge state of split-vacancy complexes

Summarizing the experimental data supported to a certain extent by theoretical calculations (with problems related to *ab initio* calculations considered in more detail in Section 6), it is possible to propose the structure of the impurity levels of split-vacancy impurity centers, schematically depicted in Fig. 10. When applied to SiV centers, it approximately corresponds to the scheme proposed in [89]. An essential role is here played by the partially filled impurity doublet E_g (hereinafter, representations of the $\bar{3}$m group are considered), which lies somewhat (by 1–1.5 eV) higher than the top of the valence band, and by the completely filled impurity doublet E_u, which lies approximately at the level of the top of the valence band. The presence of this second impurity level leads to the splitting of the triplet T_d, which in pure diamond corresponds to the top of the valence band and is transformed under a representation of the $\bar{3}$m group into a singlet A_g and a doublet E_g with a characteristic splitting energy ≈ 0.5 eV. In addition, somewhat lower in energy is located an impurity singlet A_g. The luminescence observed in the infrared range is caused mainly by the transition of electrons from the completely filled impurity level E_u to the partially filled level E_g; the calculated difference in energy between them exactly corresponds to the experimentally observed luminescence frequency. Because both levels are doublets, the experimentally observed fine splitting of the luminescence band gives a quadruplet (without taking the hyperfine splitting caused by the interaction with nuclear spins into account), and the experimental value of the splitting frequency together with the temperature dependence of the intensities of each of the four optical components allows uniquely determining the splitting for each of the electron doublets (≈ 1 meV).

We note that the optical transitions $E_u \rightarrow E_g$ are allowed by the selection rules, whereas the transitions from other adjacent levels (both impurity and purely diamond A_g and E_g) are forbidden. Nevertheless, it was shown in [89] that such levels can form a 'dark' state (shelving level), which can help in explaining the sufficiently fine features of luminescence of single impurity centers (for example, double relaxation (bunching–antibunching) in the autocorrelation function $g^2(t)$ of the SiV centers [14]) (Fig. 11).[2] Besides the

[2] *Bunching* is a radiotechnical term denoting the grouping of separate discrete signals along the time axis. The opposite tendency (a uniform distribution of separate pulses in time), which corresponds to the anti-correlation in their sequence, can then be called *antibunching*. In quantum optics, both these terms are applied to separate particles and, in the case under consideration, to photons.

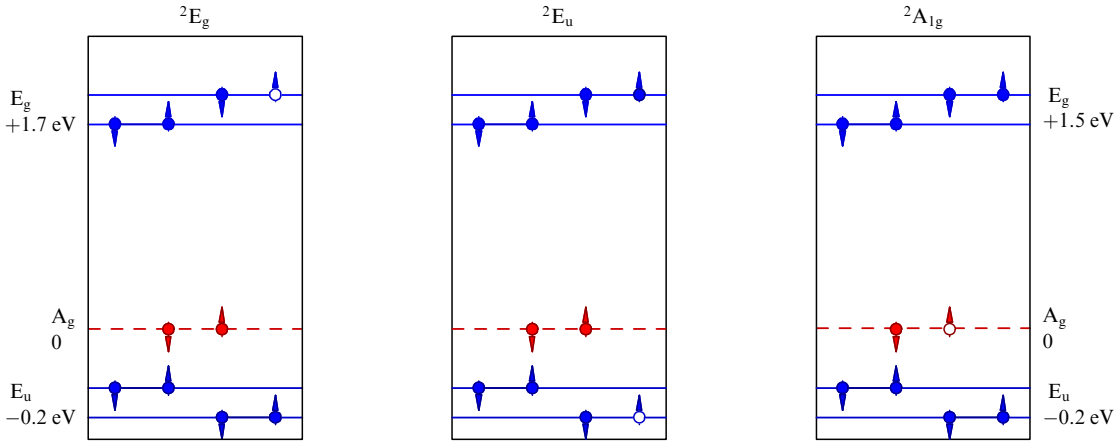

Figure 10. Schematic structure of impurity Kohn–Sham electron orbitals (solid lines) near the top of the valence band of diamond (shown by a dashed line) of the negatively charged split-vacancy complex, which corresponds to the ground (^2E_g), excited (^2E_u), and one of the possible 'dark' ($^2A_{1g}$) states [51, 89]. The values given along the vertical axes indicate the symmetry of the one-electron wave function and the corresponding energy values for the GeV^- centers (left-hand axis) and SiV^- centers (right-hand axis). The filling of the levels is shown by the white dot corresponds to the unfilled state.

fundamental value, the study of dark states is important from the standpoint of applications, where the low transition probability from the optically active excited state to this dark level is important, which means a high quantum efficiency of the single-photon emitter [8]. In the ideal case, it would be desirable, of course, if each absorbed photon were subsequently re-emitted via luminescence (with the quantum yield equal to unity). A comparative analysis of the quantum yield, the relative efficiency of the ZPL (Debye–Waller factor), the lifetime in the excited state, the counting rate, and other very important characteristics of single-photon emitters based on the SiV, NV, and other luminescent centers have been performed or measured in detail in reviews [7, 8]. As regards the GeV center, a preliminary estimate of the quantum yield [30] gives values no worse than those for the SiV center (0.05), but less than for the NV center (0.7).

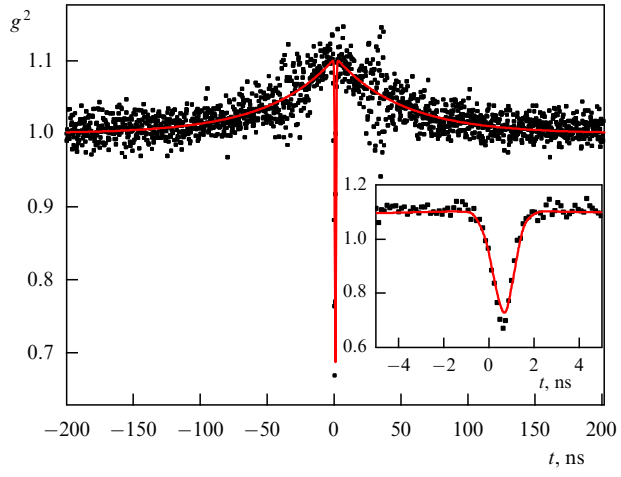

Figure 11. Autocorrelation function of a single SiV^- center (borrowed from [90]), which demonstrates the bunching–antibunching behavior described by the formula $g^2(t) = 1 - (1 + a)\exp(-|t|/\tau_1) + a\exp(-|t|/\tau_2)$, where a is the amplitude of the relaxation process, and τ_1 and τ_2 are the relaxation times of the bunching and antibunching processes. The inset shows a magnified part of the $g^2(t)$ dependence near $t = 0$. The value $g^2(t = 0) < 1$ (antibunching) indicates that this center is a single-photon emitter. The existence of a range of times where $g^2(t) > 1$ and the subsequent asymptotic decrease in $g^2(t)$ to unity (bunching) indicate the existence of a nonactive 'dark' state in this state.

When investigating the optical properties of impurity centers, it is convenient to represent the optical transitions as those between different levels described by a multielectron density function, i.e., by a molecular term. For neutral and negatively charged split-vacancy impurity complexes, such a function respectively includes six and seven single-electron states. The ground state in this case has the ^2E_g symmetry [89] for negatively charged centers and the $^3A_{1u}$ symmetry for neutral centers; the excited state has the respective ^2E_u and $^3A_{2g}$ symmetry. In this notation, the left superscript corresponds to the number of spin projections and the other indices correspond to the crystallographic symmetry of the wave function. It is important to note that the ground state of negatively charged complexes has spin 1/2 (and hence two projections, + and −), and in the case of neutral impurities, according to Hund's rule, the two electrons on the doubly degenerate upper level E_g have collinear spins, and hence the total spin is $S = 1$.

According to the Jahn–Teller theorem, a split-vacancy complex, having a doubly degenerate and partially filled level, is unstable, which leads to the removal of the degeneracy (splitting). For negatively charged centers, the following splitting energies were obtained experimentally: 0.21 meV (50 GHz) and 1.08 meV (260 GHz) for SiV^- [91, 92]; 0.75 meV (181 GHz) and 4.63 meV (1.12 THz) for GeV^- [30] for the respectively ground and excited states.

For the SiV^- center, an assumption was made that the degeneracy is lifted due to a shift of the impurity atom relative to the axis that connects the two vacancies, which leads to the disappearance of the trigonal axis and to a reduction in the symmetry of the complex to monoclinic (in essence, this is the static Jahn–Teller effect) [89]. Later experimental investigations of the Zeeman splitting [51, 91] made it possible to conclude that the splitting of the electron levels is caused by the spin–orbit coupling. But a calculation based on the DFT for the GeV^- center [30] has shown that the calculated energies of the spin–orbit coupling substantially exceed the experimental values.

It is useful to compare these data with the results obtained for the more thoroughly studied case of a negatively charged

NV center. For this center, the luminescence is caused by transitions from the completely filled single-electron singlet level A_1, which lies approximately 1 eV above the upper edge of the gap, to the partially filled (by two electrons) doublet E located 1.95 eV higher in energy (representations of the point group 3m) [93], such that these levels lie deep in the gap. The multielectron function constructed for four electrons has the $^3A_2$ symmetry for the ground state and ^3E for the excited state. This means that both these states represent a spin triplet, which also follows from Hund's rule.

Therefore, the luminescence line of the NV^- center represents a sextet [50, 94], but the splitting energy is much less than in the case of split-vacancy impurities: the fine splitting (which is ascribed to both the spin–orbit and spin–spin interactions) leads to a difference between the energies of the level with zero and nonzero projections of the spin ≈ 2.88 GHz and ≈ 10 GHz for the ground and excited states [50, 94]. Consequently, by considering transitions from the ground state with a zero or nonzero spin projection into some of the excited states with a definite projection of the orbital momentum, it is possible to realize a classical Λ system in the NV^- centers, which has remarkable prospects for being used in quantum communications and quantum computing [13, 95, 96].

To determine what charge state is realized in these impurity centers, we recall that the concentration of split-vacancy centers, in view of their very nature, is small. Because the concentration of simple impurity centers (substitutional atoms, interstitial atoms, and vacancies) is much greater, changes in the concentration of these 'simple' defects actually exert a significant effect on the position of the Fermi level of the diamond matrix, and variations in the Fermi level can in turn change the charge state of vacancy complexes. Such variations can significantly (by ≈ 0.3 eV) change the behavior of optical transitions in these centers. As was noted above, the partially filled impurity level of the SiV center lies somewhat higher than the top of the valence band. The presence of one more donor impurity, which leads to an increase in the Fermi level by approximately 1 eV above the top of the valence band, should lead to the negative charging of this impurity, and such a charge redistribution, in turn, should lead to a change in the energy structure of impurity levels.

In particular, the available experimental data indicate that the energy of luminescence for a neutral SiV center (SiV^0) has a typical value 1.32 eV, whereas the energy of luminescence of the more common (and therefore leading to a greater luminescence intensity) negatively charged center SiV^{-1} is 1.68 eV. It is precisely the SiV^{-1} line that was first revealed experimentally.

In diamond doped with germanium, the 2.06 eV line appears to correspond to a negatively charged GeV center, because the first-principle calculations for the neutral impurity give a considerably lower transition value (1.75 eV) [30]. There are no experimental papers concerning the detection of spectral lines that could be connected with the luminescence of the neutral GeV complex. Although the charge state can be sufficiently simply simulated by the DFT method, the practical matching of the specific charge state of a concrete impurity center with the observed luminescence lines can be a very nontrivial experimental problem.

Typical diagrams used for the calculation of charge states are given in Fig. 12. The energy of the formation of a defect is plotted along the vertical axis; in this case, for the C, Si, and Ge atoms, experimental values for an appropriate crystalline

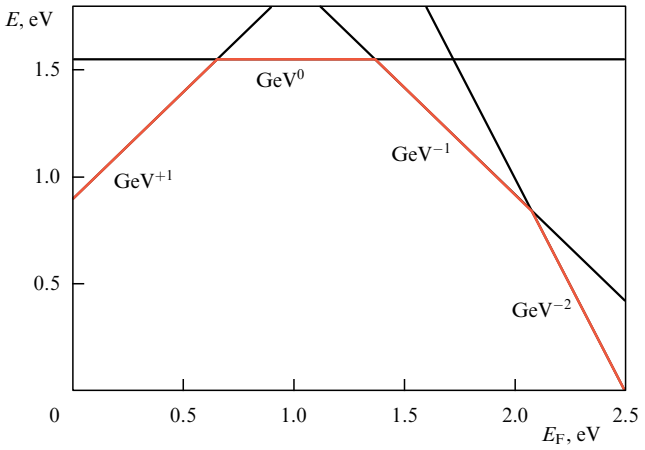

Figure 12. Diagram of the charge state of a GeV complex.

state are taken as the chemical potentials; and for the electrons, the values of the Fermi energy E_F calculated by the DFT method are adopted. It this case, it is assumed that at a certain value of E_F (corresponding to the abscissa axis in Fig. 12) in a crystal containing defects, the defect with the smallest possible energy is realized; graphically, such a diagram looks like a polygon formed by intersecting straight lines constructed for different charge states $E - E_F$. The abscissas of the vertices of this polygon determine the energy values at which a recharging (change in the charge state) of the defect occurs. As can be seen from Fig. 12, four charge states are possible for the GeV centers: 1, 0, −1, −2, but the two extreme ones are energetically stable only at unrealistic values of the Fermi energy.

5. Interaction between electron and phonon subsystems: The Huang–Rhys model

The complexity of the electron structure of impurity centers by no means exhausts the difficulty of describing impurity complexes. Experimentally observed luminescence is to a significant extent caused by the interaction of electron and phonon subsystems, in which an essential role is played by the impurity (local) phonon modes. The frequencies of oscillations of this type can also be obtained by first-principle calculations; however, there is a subtle aspect connected with the study of vibrations of an excited state. Although excited states are poorly described by such calculations, they can be explained qualitatively in the framework of a sufficiently simple Huang–Rhys model [97–99] (Fig. 13).

We note that the idea of the interaction of optical electron transitions and harmonic vibrational motions of atoms was suggested much earlier in the work of Frank [100], Condon [101], and Frenkel [102]. In the work of Huang and Rhys, who subsequently developed this idea, sideband vibrational spectra of impurity atoms (corresponding to the lines of the A and AS transitions in Fig. 13) were calculated. Although the theoretical investigation of this model can be considered to have been completed already in the 1970s, its application for the interpretation of experimental data still encounters difficulties, which can be seen, for example, from the recent mini-review [103] with practical 'recipes' for applications of this theory. Therefore, we believe it is expedient to reproduce the basic concepts of the Huang–Rhys model here.

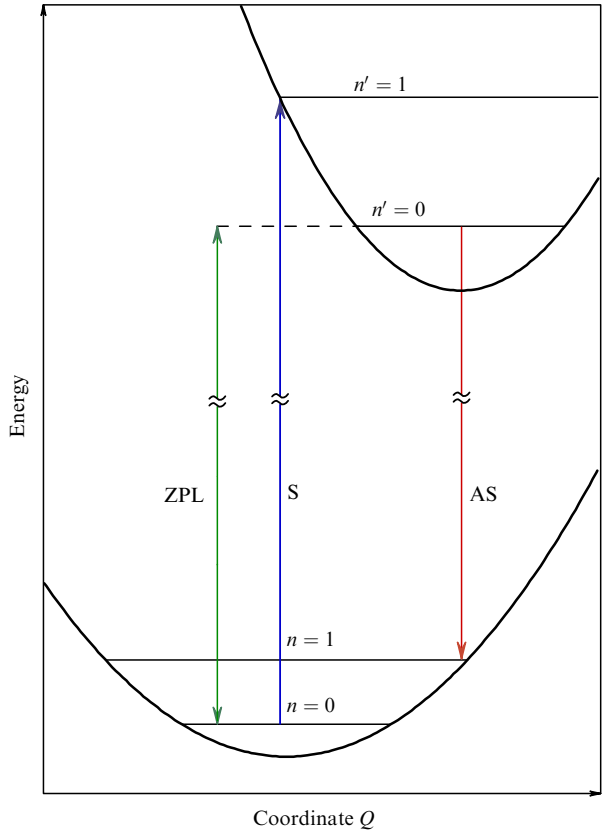

Figure 13. Huang–Rhys model (schematic). The first two vibrational levels of the ground (n) and excited (n') states are shown.

An impurity atom (or complex) in the ground state can be described as being located in a harmonic well. Thus, the quantum description of this system in the harmonic approximation leads to a set of equidistant vibrational levels. All this series nevertheless corresponds to the ground, i.e., unexcited, electron state of the impurity complex. An optical excitation of this impurity complex leads to a sufficiently strong change in the charge density near this center, such that the geometric position of the center becomes energetically unfavorable, which leads to a change in the generalized coordinate Q of this center (see Fig. 13). As the generalized coordinate, we can consider, for example, the distance from the impurity atom to the nearest carbon atom or the displacement of the impurity atom with respect to the axis that connects two adjacent vacancy sites (depending on the initial adopted model). Nevertheless, it is assumed that the electron excitation is sufficiently long-lived, such that the excited center has enough time to find an energy minimum and relax into it, before the electron passes to the ground state. Certainly, even in the case of such a metastable state, the excited center can be assumed to be located in a practically harmonic potential well with an appropriate equidistant spectrum of vibrational levels.

The optical transitions in this model are caused mainly by the transitions between two zeroth vibrational levels (corresponding to the ground and excited electronic states). In this case, the brightest luminescence line was therefore called the zero-phonon line (ZPL). At the same time, transitions between the excited vibrational levels lead to the appearance of a discrete spectrum of the so-called side band (vibronic band), observed in the region above or below the ZPL. These energy ranges correspond to absorption or luminescence, which requires substantially different experimental methods of study, with the resultant problems of combining the experimental data, for example, on the normalization of intensities [103]. It is interesting to note that the GeV^- center, clearly visible in the luminescence spectra, has not yet been registered in optical absorption [30].

Such a detailed description of these transitions is to be used in explaining the logic of quantum chemical calculations in Section 6. Furthermore, there is a quite subtle aspect connected with the comparison of the parameters of the potential well in the ground and excited states. A well-known problem in quantum chemical calculations is the fact that (by the essence of the DFT method) they are fundamentally applicable only for the calculation of the ground state energy of a certain configuration of atoms. But the calculation of mechanical vibrations in an excited electron state is an even more difficult problem. In the case under consideration, it is necessary to investigate mechanical vibrations of an excited electron structure, and it is then tempting to consider the quanta of vibrations for the excited and ground electron states equal. In essence, this amounts to the assumption that the coupling constants of the impurity complex with the surrounding diamond matrix in the excited and unexcited electron states are equal; for example, this was assumed in recent preprint [104], where the energies of the vibrational levels of the SiV complex were calculated. In the case of NV centers, the experimental data in [2] indicate that this assumption is completely justified; for split-vacancy centers, this is not the case. This problem is considered in more detail in Section 7.

The classical result of the theory of luminescence, which comes from the work of Stokes, is the difference between the wavelength of an optical excitation of the crystal structure and the wavelength of the emitted light. In the Huang–Rhys model, the two limit values of the energy of the absorbed emission are associated with the turning points [98] of the zeroth vibrational level (in Fig. 13, the 'averaged' Stokes line of the transition S, which lies in the middle between them, is shown). The difference between the energies of the absorbed and emitted light is called the Stokes losses (or the Stokes or Franck–Condon shift).

The reverse ('anti-Stokes') transition with the energy lower than the ZPL energy is observed in the luminescence spectrum. The anti-Stokes transition line that corresponds to this energy is depicted in Fig. 13 schematically. It is remarkable that this energy manifests itself in experiment in the form of a quite wide maximum observed in the luminescence spectrum near the ZPL. For the SiV^- center, this maximum with $\Delta E \approx 40$ meV relative to the ZPL line (Fig. 14) is sufficiently narrow, such that it was even interpreted previously as a local vibrational mode [4]. This value of energy had its theoretical explanation in the framework of the model of a double impurity center, to which this defect was previously ascribed [4, 106].

6. First-principle methods of calculation of vacancy complexes

In the absence of direct experimental data, the structure and the electron state of an impurity center can be estimated by comparing the values of the ZPL energy with theoretical predictions (the structure of the SiV center was determined in just this way in [46]).

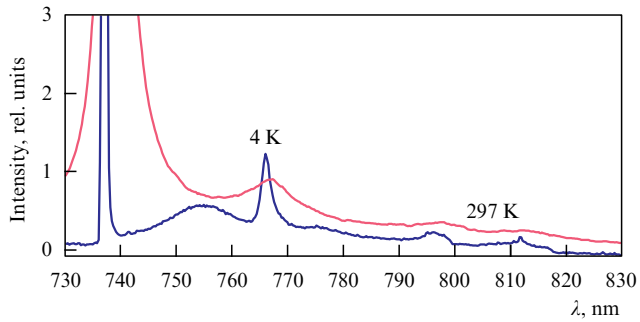

Figure 14. Luminescence spectrum of an SiV^- center at room temperature (297 K) and at the liquid helium temperature (4 K) [105]. The low-temperature spectrum exhibits three characteristic features caused by the electron-vibrational structure of the defect center: a ZPL (737 nm); the maximum of the background of the side vibronic band (755 nm); and the first vibronic line (765 nm).

There are two approaches to the calculation of the electron states of impurity centers in a crystal lattice [107]: the supercell method and the cluster method. In the first case, an individual defect is simulated by multiplying the period of the initial cell around the impurity center; in the second case, the impurity center is simulated as a separate center in a crystalline cluster, located inside an 'empty box.' The second model is apparently more suitable for a single nanocrystal, but in addition to the need of taking surface effects into account, it encounters computational difficulties due to the increased size of the computation domain (a higher cut-off energy for plane waves). In the case of split-vacancy impurity centers, a 'nanocrystal' consisting of 512 carbon atoms with a hydrogenated surface was used in [46] to calculate the optimum structure of an SiV center. In that study, an idea was also suggested that the hydrogenation of the surface compensates the known problem of the underestimated excitation energies of electrons obtained in the calculations by the LDA/GGA method (the local density approximation in the generalized gradient approximation).

At present, a conventional method for solving this problem is the 'post-processing' of the results of first-principle calculations using the Henderson–Scuseria–Ernzerhof (HSE) method, or the GW method (G is the Green's function and W is the Coulomb interaction) [108–110], which implies two methods of introducing nonlocal quantum corrections into the density functional. In the HSE method, a 'dosed' (as a rule, equal to 0.2) Fock contribution is added; and in the GW method, one-loop diagrams are taken into account. Because the simulation of single centers requires the calculation of large supercells (to the extent allowed by the accessible computational resources), the HSE method is more economical from this standpoint, although it presumably also leads to somewhat underestimated values of the energy of band gaps (by less than 0.1 eV). The calculations by the HSE method for the NV and SiV centers showed a good agreement with experiment [89, 93, 111].

The scheme used in [30] for calculating the impurity levels of the GeV centers mainly follows the one suggested in [93], with minor differences. The Quantum ESPRESSO program package [112] used in [30] for calculations by the HSE method requires that all preliminary calculations be carried out with norm-preserving pseudopotentials (this leads to an additional consumption of computational resources). The first stage of calculations is the total relaxation of the supercell (of both the coordinates of atoms and its size) with the included impurity center, taken to be in a specified charge state, with the use of an $8 \times 8 \times 8$ Monkhorst–Pack grid for averaging the energy over the Brillouin zone. The energy value thus obtained corresponds to the minimum of the unexcited state energy. Varying the charge state and analyzing the results obtained for different values of charge allows constructing a charge diagram similar to that given in Fig. 12. Comparing the electron levels calculated for the obtained coordinates of atoms and the supercell size with the electron structure of pure diamond allows identifying the impurity electron levels, thus obtaining a crude initial estimate of the energies of electron excitations. The second stage of calculations is the refinement of this value by a self-consistent calculation with the HSE method with a fixed geometry of the cell. In view of the significant computational complexity of the second stage, the averaging of energy in this case was performed only at the Γ point. The value of the calculated excitation energy at the center of the Brillouin zone is already close to experimental, and, using the difference between the initial value of the excitation energy and the refined value (which is equal to almost 0.6 eV) and simply shifting the free electron levels upward by this value (a scissors operation), it is possible to refine the diagram of electron states in the entire Brillouin zone.

We note that the value thus obtained is the energy of vertical electron excitation. In order to link it to the ZPL energy, it is necessary to subtract the Franck–Condon shift from it. Although for the split-vacancy impurity centers it turns out to be small (30 and 27 meV for the respective SiV^- center [89] and GeV^- center [29]), this is not the general case; for example, for the NV^- center, this shift has a perceptible value: 150 meV. Therefore, it is expedient to indicate the procedure for the last stage of calculations. The calculation of this shift consists in creating an inverse population density of levels and repeating the relaxation of the cell, i.e., in seeking the minimum of the energy for the excited electron state. With the use of the Quantum ESPRESSO program code, such an operation can be implemented only for one **k** vector; the vector that corresponds to the Γ point is chosen. The difference between the initial and optimized energy values gives the Stokes component of the Frank–Condon shift. By subtracting it from the energy of the vertical electron excitations, the ZPL energy is obtained. Analogously, the value of the anti-Stokes shift is determined simply by substituting the obtained optimized coordinates in the initial scheme (used at the first stage) and by running one cycle of self-consistent calculations (without varying the geometry of the cell). The decrease in the energy obtained in this cycle gives the value of the anti-Stokes shift.

A small inaccuracy was allowed above: as can be noted, the difference between the minima of the energies of electrons that are in the ground and excited states does not generally coincide with the ZPL energy (which is equal to the difference between the energies of zero vibrations). If the energy surfaces of the ground and excited states are similar (are only shifted in energy), then this correction is indeed negligible. However, it turns out that this is not the case in split-vacancy complexes; this correction, although small, is quite noticeable ($\sim$ 10 meV). How it manifests itself in experiment is discussed in Section 7.

7. Isotope effects

As was shown in Section 6, the luminescence of a defect center in diamond, in particular, its ZPL, is closely connected with the zero quasilocal vibrations of impurity atoms. Although the zero-point oscillations are a fundamental property of quantum oscillators, there are several experimental procedures that make it possible to detect the effects caused by vibrations of this type [113, 114]. The simplest (and historically the first) method that allowed confirming the existence of such effects is the study of isotope effects. As was noted in [98], the isotope shifts in a crystal vividly illustrate the fact that each line in the spectrum of the crystal is essentially an electron-vibrational line [98]. However, strange as it may seem, this method was only rarely used in studies of impurity–vacancy complexes in diamonds, mainly because the impurity atoms are introduced into the diamond matrix in a poorly controlled manner (for example, nitrogen from the atmosphere or silicon from technological equipment in the process of CVD growth) with the result that, in essence, the impurities have a natural isotope composition. Attempts previously undertaken to change the isotope composition of silicon impurity [115] in the process of CVD growth led at best to a 90% isotope enrichment with ^{29}Si because of the uncontrollable contamination by natural silicon.

We emphasize that by the isotope effects, we here mean precisely the effects caused by the isotope composition of the impurity. The effects connected with the isotope composition of the carbon matrix in pure and doped diamonds have been examined fairly often (see, e.g., [116, 117] and the references therein), mainly because of the relative simplicity of the synthesis of such samples (which, naturally, does not make the effects observed in these samples simpler; rather, the opposite is true).

A somewhat different approach was used in [118] (2014), where single SiV^- centers in CVD films were studied. Although natural silicon was used, the hyperfine splitting of a ZPL created in the spectrum was theoretically calculated for each of its isotopes. Therefore, investigating the luminescence spectrum of each single complex allowed making a conclusion on precisely which of the silicon isotopes participated in the formation of this center. By studying a sufficiently large number of single centers, it was possible to obtain data on a few isotopes at once. Of course, such studies require a very high sensitivity of the equipment employed, and therefore some fine effects are lost; however, the authors of [118] first obtained data on the isotope shifts of the ZPL and of the first two luminescent vibronic peaks of the SiV^- center. They showed that depending on the mass of the silicon isotope, the difference between the energies of the ZPL and of the first or second vibronic peaks changes as $\Delta E \sim 1/\sqrt{m}$ (Fig. 15). Taking into account that the coupling constant of the impurity with the crystalline matrix very weakly depends on the isotope mass, this result is in complete agreement with the formula for a harmonic oscillator. However, we note that the two values of the energy thus obtained, ≈ 61 and 128 meV [118], which correspond to the difference in the energies of the first and second vibrational levels relative to the zero level of the unexcited electronic state, are not strictly equidistant. This can indicate the existence of a small anharmonism of the potential well, which, on the other hand, can lead to a small deviation from the square-root dependence of the energy of the second vibrational level, which was also noted in [118].

Similar arguments were used in [30] to prove that the luminescence line at 602 nm observed in diamond grown at high pressure in the presence of isotopically pure germanium was caused precisely by germanium (see Section 3.5). Although only the first vibronic line (with the relative energy ≈ 44 meV) was examined in [30], the square-root dependence on the mass of the impurity for its energy was convincingly demonstrated for three germanium isotopes.

We recall that the density of phonon vibrations of diamond is mainly concentrated in the range 73–167 meV [4], which assigns two upper limits ('soft' and 'hard') of the

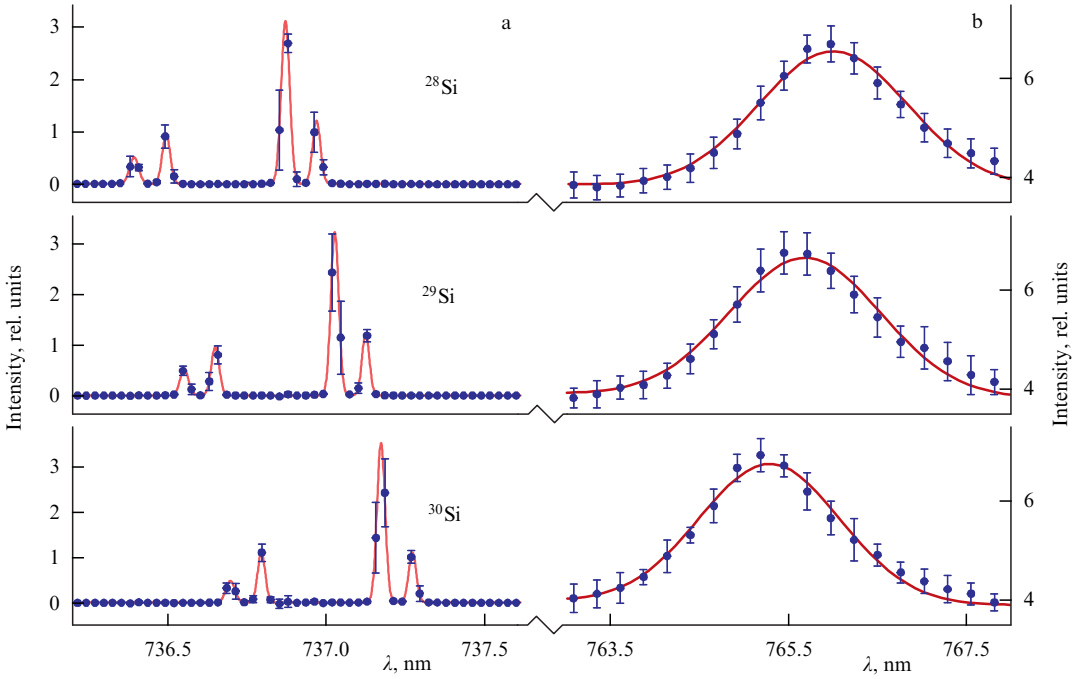

Figure 15. Isotope shift of (a) the ZPL and (b) the first vibronic peak for the SiV^- complex obtained in [105].

energy of local vibrations in the diamond lattice. The peak of the density of phonon vibrations at the upper boundary of this range is many times greater than that at the lower boundary, and hence the spectral density related to the bulk phonon modes in diamond is typically manifested in the form of a characteristic 'three-humped' structure with the peaks located at distances of 127, 157, and 167 meV from the ZPL [4]. Thus, in the case of the GeV^- and SiV^- centers, the local vibrational modes quite well fall into the 'soft window' of energies lower than 73 meV.

It is interesting to note that from a comparison of the vibrational energies (64 and 44 meV) of the SiV center and of the germanium center, based on the reasoning suggested in [4], it can be shown that both these centers are also structurally identical. Indeed, assuming that the coupling constants of each of these centers with the diamond matrix are approximately equal and each of the centers contains the same number of valence electrons (equal to seven, meaning that both centers are negatively charged), the ratio of these energies should exactly coincide with the square root of the ratio of the masses, which is satisfied to within 10% ($\sqrt{74/29} - 64/44 \approx 0.15$). This agreement can be considered good enough for such a rough model.

One more parameter can be extracted from the analysis of the isotope shift of the absolute energy of the ZPL, which was observed in both studies [30, 118]. In both cases, an increase in the isotope mass led to a small decrease in the absolute energy of the ZPL: by 0.4 meV for the $^{72}Ge - ^{76}Ge$ pair and by 0.75 meV for the $^{28}Si - ^{30}Si$ pair; the relative energy of the first vibrational level for the same pairs of isotopes respectively decreases by 1.1 and 2.2 meV. If we take Fig. 13 into consideration and assume that the difference between the energies of the minima of the potential traps for the ground and excited electron states is independent of the isotope masses (which is quite justified, because this value is determined only by the electron configuration), then the isotope shift of the ZPL allows calculating the energy of the vibration quantum of the excited electron state. For a quantum harmonic oscillator, this value should be two times greater than the relative energy of zero-point vibrations referenced to the bottom of the potential well. Thus, for the germanium center, the isotope shifts of the zero vibrational level of the respective unexcited and excited centers should be -0.55 and -0.95 meV, whence it follows that the relative energy of the first vibrational level of the excited electronic state is 76 meV. A similar reasoning for the SiV^- center gives a value of almost 107 meV. Hence, it is possible to draw the conclusion that in the excited electron state, the binding energy of the split-vacancy impurity with a diamond matrix increases significantly. This result is in striking contrast to the data for the NV^- centers, for which the results of first-principle calculations and the experimental data [2, 93] demonstrate only a small increase in the vibrational energy quantum of the excited center in comparison with the ground-state energy: by 75 and 65 meV, respectively. We note that an assumption about the connection of the isotope shift of the ZPL with the difference in the potential surfaces of the ground and excited states was made in [118]; however, no numerical estimates were given there.

In the Huang–Rhys model with identical harmonic potential wells for the ground and excited electron states, a unique kind of degeneracy exists due to the coincidence of energies of the optical transitions that occur without a change in the vibrational quantum number ($0' \to 0$, $1' \to 1$, etc.). However, this degeneracy is lifted in practice: taking the above estimates into account, we see that the $1' \to 1$ transition for the respective GeV^- and SiV^- centers has a greater energy than the $0' \to 0$ transition (the ZPL one) by 30 and 40 meV. Thus, $1' \to 1$ transitions should be observed upon excitation near the ZPL at relatively low temperatures, which make it possible to resolve them. However, it should be taken into account that the requirement that these lines be resolved simultaneously leads to their low intensity because of the small population of the $n \neq 0$ vibrational levels of the ground and excited electron states at low temperatures. Nevertheless, in all likelihood, one such line in the excitation spectrum is indeed observed in experiments [119] for the GeV^- center.

Impurity centers with a noticeable difference in the binding energies of the ground and excited states were theoretically described for the first time in [120]. A formula was proposed that connects the isotope shift of the ZPL (δZ) with the difference in the binding energies (Δ) and in the masses of the impurity isotopes (m and m'): $\delta Z = (1 - (m/m')^{1/2})\,\Delta/2$. It is difficult to say precisely what values the quantity Δ (occasionally also referred to as the frequency defect) can reach in principle, although values of 20% and greater are given for some molecules in [99].

8. Unsolved problems: charge state and electron paramagnetic resonance

As was mentioned above, determining the true charge state of an impurity can be a nontrivial experimental problem. One way to solve it is the study of splitting of the electron states in a magnetic field with the aid of the Zeeman effect or electron paramagnetic resonance (EPR).

The splitting of luminescence lines in a magnetic field (the Zeeman effect) in the case of a SiV^- center was investigated in [91], where the picture of the electron states described in Section 4 was generally confirmed: a splitting of each of the quadruple lines into two lines was observed, as should be expected for spin-1/2 states. Nevertheless, in studies with the aid of EPR, the picture becomes somewhat more ambiguous.

EPR studies of CVD diamonds doped with silicon were first performed in the early 2000s [121–124]. Although these studies were carried out, in all likelihood, on diamonds of low quality due to the imperfection of the technology in those days (it is mentioned in [122] that the basic impurity that makes the contribution to the EPR signal was hydrogen), three resonance lines caused by the impurity of silicon were nevertheless identified: a KUL1 line with spin 1 and KUL3 and KUL8 lines with spin 1/2. This made it possible to ascribe the KUL1 line to the neutral SiV complex (which was subsequently confirmed in [115, 125, 126]). However, there is no clarity regarding the negatively charged complex. It was shown that the angular dependence of the KUL3 line in the case of single crystals of CVD diamonds indicates a monoclinic (rather than trigonal) symmetry of the defect; it was therefore associated with the SiV complex and atomic hydrogen trapped by it [121, 127]. Although, as was noted in Section 4, the reduction in the symmetry to monoclinic is possible for the negative SiV complex as a result of the Jahn–Teller effect, the version with the spin–orbit nature of the electron degeneracy lifting in this complex currently seems to be more plausible. Furthermore, in recent study [126] performed on HPHT diamonds doped with silicon in a hydrogen-free medium, no presence of the KUL3 line was

noted, which suggests the participation of hydrogen in the origin of this resonance.

Thus, using the elimination approach, it is possible to conclude that it is the KUL8 line that corresponds to the SiV^- complex [123, 124], but it should be recognized that there is no direct confirmation of this (see, e.g., the discussion in [48]; the situation has not improved radically since then). An additional argument against this version can also be the fact that this EPR line is the weakest of the given series (much weaker than KUL1), which is in sharp contrast to the fact that the intensity of the luminescence of the neutral SiV complex is typically noticeably lower than that of the negatively charged complex (even in diamonds obtained by HPHT synthesis, in [126]). Judging from recent papers [128, 129], the situation is just the same in HPHT diamonds doped with germanium: an EPR line with $S = 1$ is observed (i.e., supposedly caused by the neutral GeV complex, whose presence, however, has not even been revealed in the luminescence spectrum), but no line that could be ascribed to the negatively charged impurity split-vacancy complex has been found.

We note that previously attempts were made [115, 125] to relate the absence of an appropriate $S = 1/2$ line in CVD diamonds doped with silicon to the dynamic Jahn–Teller effect, which suggests a weak splitting of the degenerate level (smaller than the energy of temperature fluctuations). In principle, this condition is satisfied in the case of both the SiV^- and GeV^- complexes. Hence, it can be assumed that in this case, the EPR measurements at temperatures of 10 K or higher lead to rapid spin fluctuations, which 'wash out' the EPR signal. Possibly, low-temperature EPR measurements will shed light on this problem, which will not only finally explain the charge state of these complexes, but also result in practical applications, because the Rabi oscillations based on this effect are widely used for the readout of spin states in quantum computing.

Photoionization of the impurity complex can serve as another method for determining the charge state (for an example of the prospects of this method in application to the NV complexes, see [130, 131]). But in contrast to the NV centers (in which the impurity levels are located almost in the center of the forbidden band), the impurity levels of split-vacancy complexes are located nearer to the valence band, which restricts the applicability of this procedure, making it somewhat one-sided: to change the charge in the positive direction, an ultraviolet laser is required, whereas for the change in the negative direction, a usual red laser is sufficient.

In this connection, we mention [132], where the characteristics of NV and SiV centers were compared and a significant tendency of SiV centers toward 'photobleaching' was noted. This result can be explained by the fact that for negatively charged split-vacancy impurity complexes, an increase in the negative charge (to -2) makes them completely inactive in the infrared and visible light ranges (both electron doublets are then completely filled).

9. Prospects for application

In all likelihood, nanodiamonds with split-vacancy impurity complexes, because of the high intensity of the ZPL in comparison with the vibronic band, can find wide application in high-resolution microscopy in medicine and biology [133, 134]. In addition, studies of single SiV centers [14] and GeV centers [27] showed that these centers are single-photon emitters. This, in particular, follows from a decrease in the autocorrelation function $g^2(t = 0) < 1$ in the region $t < 1$ ps (see Fig. 11), which indicates a low probability of the simultaneous emission of two photons (its difference from zero, according to [14], should be interpreted as a result of a measurement error).

The relative efficiency of the ZPL (Debye–Waller factor), of course, decreases with an increase in temperature, which can be seen from comparing the corresponding luminescence spectra obtained at cryogenic and room temperatures. At room temperature, the intensity of the ZPL for SiV, NV, and GeV centers in diamond is considered to be acceptable [7, 27], at least from the standpoint of obtaining single-photon emitters whose actual operation implies temperature stabilization, i.e., cooling to room or lower temperatures. For biological objects, the operating temperatures do not exceed 40–50 °C, which does not cause serious changes to the efficiency of the emitters in comparison with that at room temperature. As regards the thermal stability of the SiV, NV, and GeV optical centers, the NV centers are preserved at temperatures up to 1400 °C [61], whereas the stability of SiV and GeV centers is greater, as follows from experiments on their preparation at temperatures up to 1900 °C [135]. One additional disadvantage of NV centers is that they become unstable as the size of nanodiamonds decreases to less than 30 nm [136, 137]. For the SiV center, the stability is confirmed experimentally in nanodiamonds with a size down to several nanometers [25]. For the GeV center, the problem remains not studied thus far, although in aggregated diamonds with a size of 30–50 nm, the luminescence of the GeV center was observed earlier in [30].

Thus, it can be assumed that the above-mentioned centers can be used as single-photon sources in quantum communications and cryptography, for example, for a secure quantum transmission of secret keys using the BB84 protocol (the first protocol for the transfer of secret keys, proposed in 1984 by Bennett and Brassard) [138–140]. In addition, a clear advantage of the split-vacancy complexes is the narrowness of the ZPL realized at sufficiently 'shallow' cryogenic temperatures, which allows increasing the transmission rate in this scheme [132]. At present, the BB84 protocol is already being used in practice; but as information carriers, instead of separate photons, attenuated laser pulses are used in all realizations known to us, which makes such lines of communication fundamentally vulnerable [140]. However, when using separate photons, which makes such networks fundamentally uncrackable, such a channel, due to inevitable line losses, can be used only for data transmission at small distances (of the order of 10 m [141]) or at a very low rate. If the transmitted information is limited only to the transfer of a secret key (used for encoding another (classical) channel), which is implemented with a periodicity of several hours, then the second limitation is no longer so important. Nevertheless, in the future, the question will inevitably arise about the expansion of the bandwidth of quantum channels, which will require the creation of quantum repeaters, which are essentially the three-dimensional entangled states similar to those used in experiments on testing the Bell inequalities [142].

The key element for this is the possibility of creating entangled quantum states between the impurity center and a photon [143]. In such a scheme, the impurity center could play the role of a stationary qubit, and the photon play the role of a transmitting qubit, which would make it possible to create a distributed quantum network (the scheme of the quantum

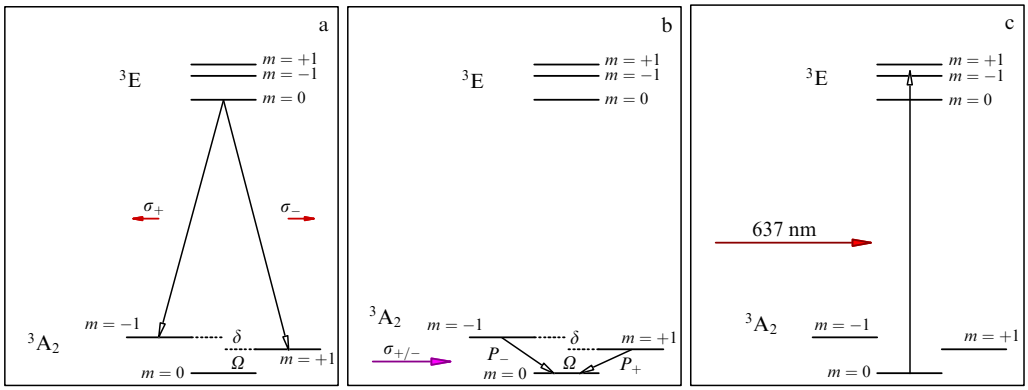

Figure 16. Creation of an entangled electron–photon state of an NV^- center in diamond according to [96]: (a) the relaxation of an excited state with the spin projection equal to zero (for details on the preparation of this pure quantum state, see [96]) can occur via two channels, accompanied by the emission of two oppositely circularly polarized photons ($\sigma_\pm$), which leads to two different spin states ($m = \pm 1$). The diagram of electron levels and transitions between the levels resembles the letter Λ in shape; therefore, this type of system was called a Λ system. The difference in the energies between the electronic sublevels of the ground state is caused by both the spin coupling ($\Omega = 2.88$ GHz) and the applied external magnetic field (δ); (b, c) the coherent readout (measurement) of the electron state, which consists of two stages: (b) the transmission of a π pulse of microwave emission with a controlled length (Rabi's cycle), which is tuned in resonance with one of the $m = \pm 1$ sublevels ($\Omega_\pm = \Omega \pm \delta/2$), leads to the passage of electrons to the $m = 0$ level with a different probability $P_+ \neq P_-$; (c) the finite population of the level $m = 0$ can be measured by means of the resonance optical excitation of this level (637 nm) with the subsequent passage to one of the electron levels with a nonzero projection of spin ($m = \pm 1$).

entanglement of photons with different directions of polarization is considered in [144]). For Λ systems, the description of the procedure of photon-spin quantum entanglement is given in [95, 145]. A demonstration of the fundamental operability of such a distributed network with a 'heralded entanglement' with the use of trapped ions is given, for example, in [146]. Because the NV^- center can be regarded as a Λ system (which in fact explains the increased attention of researchers to it) (Fig. 16), the creation of quantum-entangled states in it separated by a distance of about 1 m was demonstrated in [13, 94, 96].

The realization of such a program with the use of split-vacancy impurities meets with difficulties because the electron structure of the SiV^- and GeV^- centers is more complex (due to the double degeneracy of electron and spin states) and does not fit completely into the simple Λ system. Photon-spin quantum entanglement implies the creation of a correlated state between electron states of two types (which differ, for example, in the value of spin, as in the case of the NV^- center) and two photon states (distinguished, for example, by the polarization); moreover, the photon states should have approximately equal energies (when creating a distributed network, the photons interfere between themselves [144]).

In Refs [91, 92], it was shown that the two brightest lines in the luminescence spectrum of the SiV^- center at liquid helium temperatures (called lines A and B in [91]) with the energy splitting by ≈ 50 GHz have an orthogonal polarization, which can be used for marking the photon states of two types. These lines are caused by transitions from the lower level of the partially filled doublet E_g to some level of the E_u doublet. This system resembles a Λ system; true, in this case the electron states should be marked not with the aid of the spin but via a combination of spin and orbital states that correspond to each of the levels of the E_g doublet. In addition, each of the above levels is additionally degenerate with respect to spin, and hence difficulties arise with the procedure of coherent readout of this electron state, because the Rabi oscillations, which are standardly used for the readout of spin states [13, 94, 96, 146], can be inapplicable here.

Similar questions also arise in the case of the germanium center, but in it, in addition, the high energy of fine splitting (180 GHz) must greatly impede the interference between the photons upon the creation of a spatially entangled state. In all likelihood, these questions require additional study (see, e.g., recent studies [147, 148]), but in our opinion, the prospects for creating quantum channels based on bright and high-speed luminescent centers will compensate the efforts spent.

10. Conclusion

The analysis carried out allows selecting the HPHT synthesis as a universal tool, which is already efficiently used to improve the structure of CVD diamonds, activate impurities, and restore the structure of diamond after ion implantation, and also to modify the color grade of natural diamonds.

On the other hand, opening the possibility of the mass synthesis of doped nanodiamonds in the course of the decomposition of organic compounds at high pressures and temperatures makes the HPHT synthesis an independent and promising method for solving problems in nanoelectronics (single-photon emitters) and biomedicine (luminescent biomarkers). It has been shown that with the aid of HPHT synthesis, bright color centers can be introduced into the diamond lattice in a controlled manner. The prospects of using such centers as elements of quantum cryptography and informatics are connected with their low solubility in diamond and with the possibility of obtaining single centers in nanodiamonds with a structure (in particular, with an arbitrary isotope composition) directly in the process of HPHT synthesis. The wide forbidden band of diamond makes it possible to create quasimolecular impurity levels inside this band, which in most cases are a completely acceptable replacement for trapped single atoms, which until recently were the technological basis for studies in this field.

At the same time, in spite of the promise of this technology, a rather nonstandard situation has occurred, due to the lack of clarity as to the technological requirements regarding the color centers that can in principle be synthe-

sized in diamond. The presented requirements [8] either are trivial (the narrowness of the luminescence line and the degree of polarization of emitted light) or contradict each other. Possibly, a comparative study of the impurity–vacancy complexes that have close structures will not only help to more deeply understand the nature of optical transitions in these centers but also make it possible to set technological tasks that will subsequently allow using these centers in practice.

Acknowledgments

The authors are grateful to S M Stishov for the interest shown in our work and for the support. The authors also thank S M Stishov, V V Brazhkin, and M N Popova for the useful discussions and critical remarks expressed after reading the draft of the article, and Yu B Lebed' for the technical assistance. The work was supported in part by the Russian Foundation for Basic Research (project nos 15-02-05603 and 16-02-01120).

References

1. Clark C D, Norris C A *J. Phys. C* **4** 2223 (1971)
2. Davies G, Hamer M F *Proc. R. Soc. London A* **348** 285 (1976)
3. Zaitsev A M *Optical Properties of Diamond: a Data Handbook* (New York: Springer Science and Business Media, 2013)
4. Zaitsev A M *Phys. Rev. B* **61** 12909 (2000)
5. Zaitsev A et al. *Contrib. Gemology* **14** 41 (2014)
6. Mironov V P et al. *Russ. Geology Geophys.* **56** 729 (2015); *Geol. Geofiz.* (5) 932 (2015)
7. Pezzagna S et al. *New J. Phys.* **13** 035024 (2011)
8. Aharonovich I et al. *Rep. Prog. Phys.* **74** 076501 (2011)
9. Wrachtrup J, Jelezko F *J. Phys. Condens. Matter* **18** S807 (2006)
10. Aharonovich I, Greentree A D, Prawer S *Nature Photon.* **5** 397 (2011)
11. Balasubramanian G et al. *Nature Mater.* **8** 383 (2009)
12. Dutt M V G et al. *Science* **316** 1312 (2007)
13. Bernien H et al. *Nature* **497** 86 (2013)
14. Neu E et al. *New J. Phys.* **13** 025012 (2011)
15. Aharonovich I et al. *Phys. Rev. B* **81** 121201(R) (2010)
16. Gaebel T et al. *New J. Phys.* **6** 98 (2004)
17. Rabeau J R et al. *Nano Lett.* **7** 3433 (2007)
18. Lesik M et al. *Diamond Relat.Mater.* **56** 47 (2015)
19. Sedov V et al. *Diamond Relat. Mater.* **56** 23 (2015)
20. Ral'chenko V, Konov V *Elektronika. Nauka Tekhnol. Biznes* (4) 58 (2007)
21. Stacey A et al. *Diamond Relat. Mater.* **18** 51 (2009)
22. Petrakova V et al. *Adv. Funct. Mater.* **22** 812 (2012)
23. Chang Y R et al. *Nature Nano* **3** 284 (2008)
24. Beveratos A et al. *Eur. Phys. J. D* **18** 191 (2002)
25. Vlasov I I et al. *Nature Nano* **9** 54 (2014)
26. Rehor I, Cigler P *Diamond Relat. Mater.* **46** 21 (2014)
27. Iwasaki T et al. *Sci. Rep.* **5** 12882 (2015)
28. Ralchenko V G et al. *Bull. Lebedev Phys. Inst.* **42** 165 (2015); *Kratk. Soobshch. Fiz. Fiz. Inst. Ross. Akad. Nauk* **42** (6) 15 (2015)
29. Palyanov Y N et al. *Sci. Rep.* **5** 14789 (2015)
30. Ekimov E A et al. *JETP Lett.* **102** 701 (2015); *Pis'ma Zh. Eksp. Teor. Fiz.* **102** 811 (2015)
31. Magyar A et al. *Nature Commun.* **5** (2014)
32. Kagi H et al. *Geochim. Cosmochim. Acta* **58** 2629 (1994)
33. Kamioka H et al. *Geochem. J.* **30** 189 (1996)
34. Ueda K et al. *Diamond Relat. Mater.* **15** 1789 (2006); in *Proc. of the Joint 11th Intern. Conf. on New Diamond Science and Technology and the 9th Applied Diamond Conf., ICNDST — ADC 2006*
35. Ueda K, Kasu M *Diamond Relat. Mater.* **17** 502 (2008); in *Proc. of the Intern. Conf. on New Diamond and Nano Carbons 2007, NDNC 2007*
36. Yan C S et al. *Phys. Status Solidi A* **201** R25 (2004)
37. Charles S J et al. *Phys. Status Solidi A* **201** 2473 (2004)
38. Vagarali S S et al. "High pressure/high temperature production of colorless and fancy-colored diamonds", U.S. Patent No. 6,692,714 (2004)
39. Wang W et al. *Gems Gemology* **12** 6 (2005)
40. Vins V G, Kononov O V *Diamond Relat. Mater.* **12** 542 (2003); *13th European Conf. on Diamond, Diamond-Like Materials, Carbon Nanotubes, Nitrides and Silicon Carbide*
41. Kirillov D, Reynolds G J *Appl. Phys. Lett.* **65** 1641 (1994)
42. Khmelnitskii R A *Phys. Usp.* **58** 134 (2015); *Usp. Fiz. Nauk* **185** 143 (2015)
43. Hei L et al. *Diamond Relat. Mater.* **30** 77 (2012)
44. Wentorf R H (Jr.) *J. Phys. Chem.* **69** 3063 (1965)
45. Vavilov V S et al. *Sov. Phys. Semicond.* **14** 1078 (1980); *Fiz. Tekh. Poluprovodn.* **14** 1811 (1980)
46. Goss J P et al. *Phys. Rev. Lett.* **77** 3041 (1996)
47. Goss J P et al. *Phys. Rev. B* **72** 035214 (2005)
48. Goss J P, Briddon P R, Shaw M J *Phys. Rev. B* **76** 075204 (2007)
49. Jelezko F, Wrachtrup J *Phys. Status Solidi A* **203** 3207 (2006)
50. Doherty M W et al. *Phys. Rep.* **528** 1 (2013)
51. Hepp C J "Electronic structure of the silicon vacancy color center in diamond", Ph.D. Thesis (Saarbrucken: Univ. des Saarlandes, 2014)
52. Gibbons J F *Proc. IEEE* **60** 1062 (1972)
53. Bolduc M et al. *Phys. Rev. B* **71** 033302 (2005)
54. Seidel T E et al. *Nucl. Instrum. Meth. Phys. Res. B* **7–8** 251 (1985)
55. Uzan-Saguy C et al. *Appl. Phys. Lett.* **67** 1194 (1995)
56. Kalish R et al. *Nucl. Instrum. Meth. Phys. Res. B* **148** 626 (1999)
57. Fontaine F et al. *Diamond Relat. Mater.* **3** 623 (1994); in *Proc. of the 4th European Conf. on Diamond, Diamond-like and Related Materials*
58. Harte B, Taniguchi T, Chakraborty S *Mineralog. Mag.* **73** 201 (2009)
59. Linnarsson M K et al., in *Silicon Carbide and Related Materials 2007* (Materials Science Forum, Vol. 600–603, Eds A Suzuki et al.) (Zurich: Trans. Tech. Publ., 2009) p. 453
60. Pezzagna S et al. *New J. Phys.* **12** 065017 (2010)
61. Orwa J O et al. *J. Appl. Phys.* **109** 083530 (2011)
62. Sung J C, Lin J *Diamond Nanotechnology: Syntheses and Applications* (Singapore: Pan Stanford, 2009)
63. Sittas G et al. *Diamond Relat. Mater.* **5** 866 (1996); *Proc. of the 6th European Conf. on Diamond, Diamond-like and Related Materials*
64. Clark C D et al. *Phys. Rev. B* **51** 16681 (1995)
65. Bovernkerk H P et al. *Nature* **184** 1094 (1959)
66. Akaishi M, Kanda H, Yamaoka S *Science* **259** 1592 (1993)
67. Astakhov M, Ziganshina R, Shalimov M *Izv. Vissh. Uchebn. Zaved. Chernaya Metallurg.* (3) 15 (1993)
68. Ekimov E A et al. *Nature* **428** 542 (2004)
69. Yamaoka S et al. *J. Cryst. Growth* **125** 375 (1992)
70. Fang L, Ohfuji H, Irifune T *J. Nanomater.* **2013** 201845 (2013)
71. Kanda H, Akaishi M, Yamaoka S *Appl. Phys. Lett.* **65** 784 (1994)
72. Ekimov E A et al. *Instrum. Exp. Tech.* **47** 276 (2004); *Prib. Tekh. Eksp.* (2) 157 (2004)
73. Irifune T et al. *Nature* **421** 599 (2003)
74. Davydov V A et al. *JETP Lett.* **99** 585 (2014); *Pis'ma Zh. Eksp. Teor. Fiz.* **99** 673 (2014)
75. Kanda H, Lawson S *Industr. Diamond Rev.* **55** 56 (1995)
76. Heyer S et al. *ACS Nano* **8** 5757 (2014)
77. Mandal S et al. *Nanotechnology* **21** 195303 (2010)
78. Ekimov E A et al. *Adv. Mater.* **27** 5518 (2015)
79. Onodera A, Suito K, Morigami Y *Proc. Jpn. Acad. B* **68** 167 (1992)
80. Jantzen U et al. *New J. Phys.* **18** 073036 (2016); arxiv:1602.03391
81. Ekimov E A et al. *Phys. Status Solidi A* **213** 2582 (2016)
82. Bundy F P *J. Chem. Phys.* **38** 631 (1963)
83. Sumiya H *SEI Tech. Rev.* **74** 15 (2012)
84. Onodera A, Suito K, in *Science and Technology of High Pressure. Proc. of the Intern. Conf. on High Pressure Sciene and Technology, AIRAPT-17, Honolulu, Hawaii, 25–30 July, 1999* (Eds M H Manghnani, W J Nellis, M F Nicol) (Hyderabad, India: Univ. Press, 2000)
85. Davydov V et al. *Carbon* **90** 231 (2015)
86. Le Guillou C et al. *Carbon* **45** 636 (2007)
87. Shiomi H, Nishibayashi Y, Shikata S I "Semiconductor laser comprising rare-earth metal-doped diamond", U.S. Patent No. 5,812,573 (1998)

88. Malashkevich G E et al. *JETP Lett*. **77** 291 (2003); *Pis'ma Zh. Eksp. Teor. Fiz*. **77** 341 (2003)
89. Gali A, Maze J R *Phys. Rev. B* **88** 235205 (2013)
90. Neu E et al., arXiv:1008.4736
91. Hepp C et al. *Phys. Rev. Lett*. **112** 036405 (2014)
92. Rogers L J et al. *Phys. Rev. B* **89** 235101 (2014)
93. Gali A et al. *Phys. Rev. Lett*. **103** 186404 (2009)
94. Batalov A et al. *Phys. Rev. Lett*. **102** 195506 (2009)
95. Simon C, Irvine W T M *Phys. Rev. Lett*. **91** 110405 (2003)
96. Togan E et al. *Nature* **466** 730 (2010)
97. Huang K, Rhys A *Proc. R. Soc. London A* **204** 406 (1950)
98. Rebane K K *Impurity Spectra of Solids. Elementary Theory of Vibrational Structure* (New York: Plenum Press, 1970); Translated from Russian: *Elementarnaya Teoriya Kolebatel'noi Struktury Spektrov Primesnykh Tsentrov Kristallov* (Moscow: Nauka, 1968)
99. Sheka E F *Sov. Phys. Usp*. **14** 484 (1972); *Usp. Fiz. Nauk* **104** 593 (1971)
100. Franck J, Dymond E G *Trans. Faraday Soc*. **21** 536 (1926)
101. Condon E U *Phys. Rev*. **32** 858 (1928)
102. Frenkel J *Phys. Rev*. **37** 17 (1931)
103. de Jong M et al. *Phys. Chem. Chem. Phys*. **17** 16959 (2015)
104. Londero E et al., arXiv:1605.02955
105. Dietrich A et al., arXiv:1407.7137
106. Lin-Chung P J *Phys. Rev. B* **50** 16905 (1994)
107. Freysoldt C et al. *Rev. Mod. Phys*. **86** 253 (2014)
108. Van de Walle C G, Janotti A, in *Advanced Calculation for Defects in Materials. Electronic Structure Methods* (Eds A Alkauskas et al.) (New York: Wiley-VCH, 2011) p. 1
109. Umari P et al., in *Advanced Calculation for Defects in Materials. Electronic Structure Methods* (Eds A Alkauskas et al.) (New York: Wiley-VCH, 2011) p. 61
110. Henderson T M, Paier J, Scuseria G E, in *Advanced Calculation for Defects in Materials. Electronic Structure Methods* (Eds A Alkauskas et al.) (New York: Wiley-VCH, 2011) p. 97
111. Gali A, Fyta M, Kaxiras E *Phys. Rev. B* **77** 155206 (2008)
112. Giannozzi P et al. *J. Phys. Condens. Matter* **21** 395502 (2009)
113. Stishov S M *Phys. Usp*. **44** 285 (2001); *Usp. Fiz. Nauk* **171** 299 (2001)
114. Tsipenyuk Yu M *Phys. Usp*. **55** 796 (2012); *Usp. Fiz. Nauk* **182** 855 (2012)
115. Edmonds A M et al. *Phys. Rev. B* **77** 245205 (2008)
116. Davies G *Phys. B* **273–274** 15 (1999)
117. Enkovich P V et al. *Phys. Rev. B* **93** 014308 (2016)
118. Dietrich A et al. *New J. Phys*. **16** 113019 (2014)
119. Ekimov E A et al. *Phys. Rev. B* **95** 094113 (2017)
120. Keil T H *Phys. Rev*. **140** A601 (1965)
121. Iakoubovskii K et al. *Diamond Relat. Mater*. **12** 511 (2003); *13th European Conf. on Diamond, Diamond-Like Materials, Carbon Nanotubes, Nitrides and Silicon Carbide*
122. Iakoubovskii K, Stesmans A *J. Phys. Condens. Matter* **14** R467 (2002)
123. Iakoubovskii K, Stesmans A *Phys. Rev. B* **66** 195207 (2002)
124. Iakoubovskii K et al. *Phys. Status Solidi A* **193** 448 (2002)
125. D'Haenens-Johansson U F S et al. *Phys. Rev. B* **84** 245208 (2011)
126. Nadolinny V et al. *Phys. Status Solidi A* **212** 2460 (2015)
127. Thiering G, Gali A *Phys. Rev. B* **92** 165203 (2015)
128. Komarovskikh A Y et al. "Characterization of Ge-containing defect in diamond", in *21st Hasselt Diamond Workshop 2016, SBDD XXI, March 9–11, 2016, Hasselt, Belgium*; http://ppt-online.org/38143
129. Nadolinny V et al. *Phys. Status Solidi A* **213** 2623 (2016)
130. Aslam N et al. *New J. Phys*. **15** 013064 (2013)
131. Siyushev P et al. *Phys. Rev. Lett*. **110** 167402 (2013)
132. Leifgen M et al. *New J. Phys*. **16** 023021 (2014)
133. McGuinness L, in *Quantum Information Processing with Diamond. Principles and Applications* (Eds S Prawer, I Aharonovich) (Amsterdam: Elsevier, Woodhead Publ., 2014) p. 219
134. Fox K, Prawer S, in *Quantum Information Processing with Diamond. Principles and Applications* (Eds S Prawer, I Aharonovich) (Amsterdam: Elsevier, Woodhead Publ., 2014) p. 291
135. Palyanov Y N et al. *Cryst. Growth Design* **16** 3510 (2016)
136. Bradac C et al. *Nano Lett*. **9** 3555 (2009)
137. Barnard A, Sternberg M *Diamond Relat. Mater*. **16** 2078 (2007); in *Proc. of the Joint Intern. Conf. Nanocarbon and Nanodiamond 2006*
138. Bennett C H, Brassard G *Proc. IEEE Int. Conf. Comput. Syst. Signal* **175** 8 (1984)
139. Weinfurter H, in *Quantum Information Processing with Diamond. Principles and Applications* (Eds S Prawer, I Aharonovich) (Amsterdam: Elsevier, Woodhead Publ., 2014) p. 21
140. Neu E, Becher C, in *Quantum Information Processing with Diamond. Principles and Applications* (Eds S Prawer, I Aharonovich) (Amsterdam: Elsevier, Woodhead Publ., 2014) p. 127
141. Beveratos A et al. *Phys. Rev. Lett*. **89** 187901 (2002)
142. Aspect A, in *Quantum (Un)Speakables. From Bell to Quantum Information* (Berlin: Springer, 2002) p. 119
143. Dutt G, Momeen M, in *Quantum Information Processing with Diamond. Principles and Applications* (Eds S Prawer, I Aharonovich) (Amsterdam: Elsevier, Woodhead Publ., 2014) p. 195
144. Mattle K et al. *Phys. Rev. Lett*. **76** 4656 (1996)
145. Bliniv B B et al. *Nature* **428** 153 (2004)
146. Schug M et al. *Phys. Rev. Lett*. **110** 213603 (2013)
147. Rogers L J et al. *Phys. Rev. Lett*. **113** 263602 (2014)
148. Becker J N et al. *Nature Commun*. **7** 13512 (2016)